



e1  
RM E52D17

NACA RM E52D17



# RESEARCH MEMORANDUM

EXPERIMENTAL INVESTIGATION OF AVERAGE HEAT-TRANSFER AND  
FRICTION COEFFICIENTS FOR AIR FLOWING IN CIRCULAR TUBES  
HAVING SQUARE-THREAD-TYPE ROUGHNESS

By Eldon W. Sams

Lewis Flight Propulsion Laboratory  
Cleveland, Ohio

NATIONAL ADVISORY COMMITTEE  
FOR AERONAUTICS  
WASHINGTON

LIBRARY COPY

June 27, 1952

OCT 14 1958

RESEARCH CENTER  
NATIONAL AERONAUTICS AND SPACE ADMINISTRATION  
LANGLEY FIELD, VIRGINIA

## NATIONAL ADVISORY COMMITTEE FOR AERONAUTICS

RESEARCH MEMORANDUM

EXPERIMENTAL INVESTIGATION OF AVERAGE HEAT-TRANSFER AND FRICTION  
COEFFICIENTS FOR AIR FLOWING IN CIRCULAR TUBES HAVING  
SQUARE-THREAD-TYPE ROUGHNESS

By Eldon W. Sams

## SUMMARY

An investigation of forced-convection heat transfer and associated pressure drops was conducted with air flowing through electrically heated Inconel tubes having various degrees of square-thread-type roughness, an inside diameter of 1/2 inch, and a length of 24 inches. Data were obtained for tubes having conventional roughness ratios (height of thread/radius of tube) of 0 (smooth tube), 0.016, 0.025, and 0.037 over ranges of bulk Reynolds numbers up to 350,000, average inside-tube-wall temperatures up to 1950° R, and heat-flux densities up to 115,000 Btu per hour per square foot.

The experimental data showed that both heat transfer and friction increased with increase in surface roughness, becoming more pronounced with increase in Reynolds number; for a given roughness, both heat transfer and friction were also influenced by the tube wall-to-bulk temperature ratio.

Good correlation of the heat-transfer data for all the tubes investigated was obtained by use of a modification of the conventional Nusselt correlation parameters wherein the mass velocity in the Reynolds number was replaced by the product of air density evaluated at the average film temperature and the so-called friction velocity; in addition, the physical properties of air were evaluated at the average film temperature.

The isothermal friction data for the rough tubes, when plotted in the conventional manner, resulted in curves similar to those obtained by other investigators; that is, the curve for a given roughness breaks away from the Blasius line (representing turbulent flow in smooth tubes) at some value of Reynolds number, which decreases with increase in surface roughness, and then becomes a horizontal line (friction coefficient independent of Reynolds number).

A comparison of the friction data for the rough tubes used herein indicated that the conventional roughness ratio is not an adequate measure of relative roughness for tubes having a square-thread-type element. The present data, as well as those of other investigators, were used to isolate the influence of ratios of thread height to width, thread spacing to width, and the conventional roughness ratio on the friction coefficient.

A fair correlation of the friction data was obtained for each tube with heat addition when the friction coefficient and Reynolds number were defined on the basis of film properties; however, the data for each tube retained the curve characteristic of that particular roughness. The friction data for all the rough tubes could be represented by a single line for the complete turbulence region by incorporating a roughness parameter in the film correlation. No correlation was obtained for the region of incomplete turbulence.

### INTRODUCTION

The results of a systematic investigation to obtain surface-to-fluid heat-transfer and associated pressure-drop data with air flowing through smooth tubes over wide ranges of surface temperature and heat-flux density are presented in references 1 to 5. The investigation reported herein represents an extension of these data to the case of air flowing through rough tubes.

The available literature on fluid flow in rough tubes provides extensive friction data for incompressible flow with no heat transfer in tubes having various types of random roughness (that is, various types of commercial pipes); to a more limited extent, data are also available for tubes having various types of artificial roughness such as the Nikuradse sand-grain tubes of reference 6. On the basis of these data, von Kármán has established suitable friction-factor relations for flow in smooth pipes, and in rough pipes where the roughness is sufficient to result in completely turbulent flow. The von Kármán function for rough pipes, which is based on the data for artificial sand-grain roughness, is further shown in reference 7 to be valid for most types of random roughness. These data, based on a granular-type roughness and applicable to random-type roughness, would not be expected, however, to apply to a square-thread type of roughness where an entirely different kind of flow mechanism would occur. For the case of heat addition both friction and heat-transfer data are extremely limited in rough-tube literature; moreover, these data were obtained, in most cases, for flow of incompressible fluids in rough tubes at low values of surface temperature and heat-flux density.

The investigation reported herein was undertaken at the NACA Lewis laboratory to provide experimental heat-transfer and friction data for flow of a compressible fluid through threaded tubes over wide ranges of surface temperatures and heat-flux densities. The tests reported herein were conducted with air flowing through electrically heated Inconel tubes having various degrees of square-thread-type roughness, an inside diameter of 1/2 inch, and an effective heat-transfer length of 24 inches.

Data were obtained for three degrees of thread-type roughness; the roughness in each case consisted of a series of approximately square threads machined into the tube inner wall at essentially right angles to the direction of flow. The thread and pitch dimensions were varied from tube to tube, resulting in conventional roughness ratios (height of thread/radius of tube) of 0.016, 0.025, and 0.037. Data were also obtained for a smooth tube for comparison herein with the rough-tube results, and the smooth-tube results of references 1 to 5. The investigation reported herein covered ranges of bulk Reynolds numbers up to 350,000, average inside-tube-wall temperatures up to 1950° R, and heat-flux densities up to 115,000 Btu per hour per square foot of heat-transfer area, for an inlet-air temperature of 540° R.

#### APPARATUS

A schematic diagram of the test section and related components of the air and electrical systems used in this investigation is shown in figure 1.

##### Air and Electrical Systems

Air system. - As indicated in figure 1, compressed air was supplied to the inlet tank through a pressure-regulating valve, a filter, and two A.S.M.E. type flat-plate orifices connected in series. From the inlet tank, air passed through the inlet extension, the test section, and the mixing tank, and was then discharged to atmosphere. The inlet tank, mixing tank, and tank extensions supporting the test section were thermally insulated.

The temperature of the air entering the test section was measured by two parallel-connected chromel-alumel thermocouples located in the inlet tank. The temperature of the air leaving the test section was measured in the same manner immediately downstream of the mixing baffles.

Electrical system. - Electric power from a 208-volt, 60-cycle line was supplied to the test section (see fig. 1) through two saturable reactors and a power transformer. A voltage regulator, controlling the direct-current supply to the reactors, maintained close voltage regulation at the primary of the power transformer for any setting

(test-section input) of the variable transformer control. The capacity of the electrical equipment was 25 kilovolt-amperes at a maximum of 10 volts across the test section.

#### Test Section

Installation. - A typical test-section (rough tube) installation is shown schematically in figure 2. The test section consists of an Inconel tube having an outside diameter of 0.68 inch and a wall thickness of about 0.090 inch. An Inconel flange, welded to each end of the test section, is connected by bus bars to the power supply providing resistance heating of the tube. The distance between outer faces of the tube flanges is 24 inches, which was taken as the effective heat-transfer length. An extension (with flange) was provided at each end of the test section and the entire assembly was line-bored and doweled between flanges to maintain bore alignment. The inlet and exit extensions had lengths of 6 and 3 inches, respectively, thus providing a 12-diameter approach to the test section.

External heat losses were reduced by jacketing the test section with three concentric radiation shields with the annular spaces between the shields filled with insulating sand. An insulator, located at each end of the test-section assembly, provided electrical insulation for the test section.

Three static-pressure taps, located 120° apart around the extension flanges, were provided at each end of the test section. Outside-tube-wall temperatures were measured by use of 12 chromel-alumel thermocouples peened to the test-section wall, as shown in figure 2, with one additional thermocouple imbedded in each of the test-section tube flanges.

Preparation of roughness. - Artificially roughened tubes are generally prepared by either some form of machine cutting of the inner surface or coating of the tube bore with a granular material (such as sand) by use of an adhesive bond. When heat-transfer data are required, the latter method is undesirable because it requires the use of an adhesive layer having unknown thermal properties; this method also makes uncertain the attainment of a uniform roughness throughout the tube bore. Hence, the machine-cutting method was used in the present investigation.

A separate tube for each degree of roughness was prepared by turning a specially fabricated double-thread tap through the tube bore. The thread and pitch dimensions for the various square-thread taps were selected so as to provide the desired range of conventional roughness ratio.

In order to obtain a roughness specimen for each of the rough tubes, the tubes were tapped in 26-inch lengths; a 2-inch length was then cut from the tap-exit end of each tube, and a section of this sample was mounted and photographed to X50 magnification to show the roughness profile. The profiles for two of the rough tubes used in this investigation, herein designated as tubes A and B, are shown in figure 3 along with the corresponding thread measurements. Tube C (not shown) was later obtained by carefully honing the bore of tube A to provide a lower degree of roughness. Inasmuch as the bore for tube C had a slightly increasing taper toward either end, the diameter was measured by means of a series of short plug gages ground to differences in diameter of 0.0005 inch. By measuring the depth of insertion for each plug, a curve of bore diameter against position along the tube was plotted and integrated to obtain a mean bore diameter. The corresponding thread measurements for tube C are shown in figure 3.

#### PROCEDURE

The experimental procedure used in obtaining the data reported herein was briefly as follows: For a given average surface temperature, the air flow through the test section was adjusted to provide the desired Reynolds number; when conditions were fully stabilized, the data were recorded. Data were similarly obtained for a range of Reynolds numbers by adjusting the power input to maintain the same average surface temperature. The same procedure was then repeated for each desired surface temperature level and, in turn, for each of the tubes investigated.

#### METHOD OF CALCULATION

Physical properties of air. - The physical properties of air used in the present investigation are shown in figure 4 as functions of temperature. The curves are plotted from the data of references 8 and 9 and are the same as those used in references 1 to 5.

Evaluation of tube diameter. - The inside diameter  $D$  (all symbols are defined in the appendix) for a rough tube may be expressed in various ways. The resulting variation in the value of  $D$  can materially affect the data, particularly in the case of the friction coefficient, which varies as the fifth power of the diameter. The value of the diameter most generally used in rough-tube work is expressed by the relation

$$D = \sqrt[4]{\left(\frac{\text{Volume of tube}}{L}\right) \frac{4}{\pi}} \quad (1)$$

which is the value resulting from an internal volumetric measurement of the tube. In the present investigation, however, the inside diameter  $D$

is taken as the average of the thread-flat (minimum tube) diameter and the thread-root (maximum tap) diameter. The latter value of diameter differs from a calculated volume diameter by less than 1/2 percent for the rough tubes used herein and hence may be considered equivalent to the measured volume diameter of equation (1).

Evaluation of surface temperature. - The average inside-tube-wall temperature  $T_s$  was taken as the average outside-tube-wall temperature  $T_o$  obtained from integrated axial-temperature-distribution curves of measured local outside-tube-wall temperature (area under the curve divided by the effective heat-transfer length) minus the temperature drop through the tube wall computed from the relation (reference 10)

$$T_s = T_o - \frac{Q}{2\pi L k_t (r_o^2 - r_i^2)} \left[ r_o^2 \ln \left( \frac{r_o}{r_i} \right) - \left( \frac{r_o^2 - r_i^2}{2} \right) \right] \quad (2)$$

for heat conduction through a tube wall in which heat is generated uniformly within the wall and the heat flow is radially inward. Equation (2) may be written for any one tube as

$$T_s = T_o - C \frac{Q}{k_t} \quad (3)$$

In the evaluation of the constant  $C$  in equation (3), the outside radius  $r_o$  was 0.340 inch for all the tubes investigated, and the inside radius  $r_i$  was taken as half the inside diameter defined in equation (1). The values used for thermal conductivity of Inconel  $k_t$  are the same as those used in references 1 and 4.

Heat-transfer coefficients. - The average heat-transfer coefficient  $h$  is computed from the experimental data by the relation

$$h = \frac{W c_{p,b} (T_2 - T_1)}{S (T_s - T_b)} \quad (44)$$

The air bulk temperature  $T_b$  is taken as the average of the tube inlet-air and exit-air total temperatures  $T_1$  and  $T_2$ , respectively. The heat-transfer area  $S$  is based on the inside tube diameter as defined in equation (1). Correlation of the heat-transfer coefficients obtained herein is discussed under the section RESULTS AND DISCUSSION.

Friction coefficients. - The method used herein for computing friction coefficients is essentially as follows: The friction pressure drop is obtained by subtracting the calculated momentum pressure drop from the measured value of over-all static-pressure drop across the heater tube, or

$$\Delta p_{fr} = \Delta p - \frac{G^2 R}{g} \left( \frac{t_2}{P_2} - \frac{t_1}{P_1} \right) \quad (5)$$

The average bulk friction coefficient  $f_b$  is then computed by the relation

$$f_b = \frac{\Delta p_{fr}}{4 \frac{L}{D} \frac{\rho_{av} V_b^2}{2g}} \quad (6)$$

with the average density taken as

$$\rho_{av} = \frac{1}{R} \left( \frac{P_1 + P_2}{t_1 + t_2} \right) \quad (7)$$

The modified film friction coefficient  $f_f$ , also used herein, is computed by the relation

$$f_f = \frac{\Delta p_{fr}}{4 \frac{L}{D} \frac{\rho_f V_b^2}{2g}} = \frac{2T_f}{t_1 + t_2} f_b \quad (8)$$

Correlation of the friction coefficients obtained herein with heat addition, and also without heat addition, is discussed under the section RESULTS AND DISCUSSION.

## RESULTS AND DISCUSSION

### Correlation of Heat-Transfer Coefficients

The methods used herein for correlation of the heat-transfer data are as follows:

Conventional correlation based on bulk temperature. - The average heat-transfer coefficients obtained herein for the smooth tube are presented in the conventional manner in figure 5(a), wherein Nusselt number divided by Prandtl number to the 0.4 power  $(hD/k_b)/(c_{p,b}\mu_b/k_b)^{0.4}$  is plotted against Reynolds number  $DG/\mu_b$  with the physical properties of air evaluated at the air bulk temperature. Included for comparison is the line (dashed) which in reference 11 was found to best represent the smooth-tube data of various investigators.

With the use of the conventional method of correlation (fig. 5(a)), the data form a series of parallel lines having a common slope of 0.80 above a Reynolds number of about 20,000. Each line represents the data for a different surface temperature level investigated, for which the average values of  $T_s$  and  $T_s/T_b$  are tabulated. The data fall progressively below the reference line with increase in  $T_s/T_b$ , as was also found for the smooth-tube investigations of references 1 to 5.

The data for rough tube A, obtained at the same surface temperature levels and plotted in the same manner as that for the smooth tube, are shown in figure 5(b). In comparison with the smooth-tube results, the data for rough tube A show that an increase in surface roughness results in an increase in the rate of data separation with  $T_s/T_b$ . Moreover, the increase in roughness results in an increase in slope of the data lines, the slope increasing from 0.80 for the smooth tube to 0.90 for rough tube A. The effect of surface roughness on the increase in slope of the line is better studied in a later figure (fig. 6(b)) where the effect of  $T_s/T_b$  has been eliminated. The data for rough tubes B and C (not shown) showed similar effects of  $T_s/T_b$  and surface roughness, the results being intermediate to those of figures 5(a) and 5(b).

Modified correlation based on surface temperature. - Average heat-transfer coefficients for the smooth tube are presented in figure 6(a) with the coordinates of figure 5(a) modified as follows: Nusselt number divided by Prandtl number to the 0.4 power  $(hD/k_s)/(c_{p,s}\mu_s/k_s)^{0.4}$  is plotted against a Reynolds number in which the conventional mass velocity  $G$  (or  $\rho_b V_b$ ) has been replaced by  $\rho_s V_b$ , the product of air density evaluated at the average inside-tube-wall temperature and air velocity evaluated at the average bulk temperature. In addition, the physical properties of air are evaluated at the average inside-tube-wall temperature  $T_s$ . Included, for comparison, in figure 6(a) is the line (dashed) which best represents the data of references 3 and 4 for smooth platinum and Inconel tubes, respectively. The equation of the reference line above a Reynolds number of 10,000 is

$$\frac{hD}{k_s} = 0.023 \left( \frac{\rho_s V_b D}{\mu_s} \right)^{0.8} \left( \frac{c_{p,s} \mu_s}{k_s} \right)^{0.4} \quad (9)$$

The reference line shows good agreement with the smooth-tube data of this investigation.

The data for rough tubes A, B, and C, with the same coordinates as in figure 6(a), are presented in figure 6(b) along with the mean line (dashed) representing the smooth-tube data of figure 6(a) and equation (9). This method of plotting successfully eliminates the

effect of  $T_s/T_b$  for each of the rough tubes, thus enabling a study of the effects of roughness. Figure 6(b) shows that an increase in surface roughness results in an increase in the heat-transfer parameter which becomes more pronounced with increase in Reynolds number; at Reynolds numbers below about 3000 there is no visible effect of roughness on the value of the heat-transfer parameter. This suggests that at the lower Reynolds numbers the boundary layer is thicker than the height of roughness in each case and hence the roughness does not substantially influence the heat-transfer mechanism. At the higher Reynolds numbers, however, the boundary-layer thickness decreases to a point where the height of roughness does noticeably affect the heat transfer. The slope of the data lines increased from 0.80 for the smooth tube to 0.95 for rough tube A. The data for rough tube B, having a slope of 0.92, suggest the same over-all degree of roughness as tube A; whereas the data for tube C, having a slope of 0.84, do not differ appreciably from those for the smooth tube. These results for tubes A and B would indicate, from a comparison of the conventional roughness ratios, that factors other than roughness height are involved in evaluating the over-all roughness for threaded tubes.

The equation of the straight line through the data of rough tube A is

$$\frac{hD}{k_s} = 0.0070 \left( \frac{\rho_s V_b D}{\mu_s} \right)^{0.95} \left( \frac{c_{p,s} \mu_s}{k_s} \right)^{0.4} \quad (10)$$

while that for rough tube B is

$$\frac{hD}{k_s} = 0.0087 \left( \frac{\rho_s V_b D}{\mu_s} \right)^{0.92} \left( \frac{c_{p,s} \mu_s}{k_s} \right)^{0.4} \quad (11)$$

and that for rough tube C is

$$\frac{hD}{k_s} = 0.016 \left( \frac{\rho_s V_b D}{\mu_s} \right)^{0.84} \left( \frac{c_{p,s} \mu_s}{k_s} \right)^{0.4} \quad (12)$$

Although this method of plotting results in a good correlation of the heat-transfer data for each of the tubes investigated, it does not enable correlation of the data for all degrees of roughness.

Modified correlation based on film temperature. - In the experimental smooth-tube investigations of references 1 to 5, it was found that for best correlation of the heat-transfer data the temperature to be used in evaluating the correlation parameters was the surface temperature. In a theoretical investigation of reference 12, however, for the case of

turbulent flow of a fluid (Prandtl number of 1) in smooth tubes with heat addition over a wide range of tube wall-to-bulk temperature ratios, it was found that for best correlation of local heat-transfer coefficients the temperature to be used was one close to the film temperature; the latter results were obtained using a variation of thermal conductivity of air with temperature slightly different from that of references 1 to 4.

In order to compare the results of the present investigation, when the film and surface temperatures are used, the data for the smooth tube (fig. 6(a)) are replotted in figure 7, wherein the conventional plotting parameters are modified to the following extent: Nusselt number divided by Prandtl number to the 0.4 power  $(hD/k_f) / \left( \frac{c_p, f^{1/4}}{k_f} \right)^{0.4}$  is plotted against a Reynolds number in which the mass velocity  $G$  (or  $\rho_b V_b$ ) is replaced by  $\rho_f V_b$ , the product of air density evaluated at the average film temperature and air velocity evaluated at the average bulk temperature. Also, the physical properties of air are evaluated at the average film temperature  $T_f$ . This method of plotting, with the correlation parameters evaluated at the film temperature, results in a good correlation of the smooth-tube data.

The data for rough tubes A, B, and C, when plotted in this manner (not shown), gave similar results to that of figure 7; as might be expected, however, the separation of data with  $T_s/T_b$  increased slightly with increase in surface roughness, the separation being the greatest for rough tube A (about 15 percent). Again, as in the modified surface correlation of figure 6(b), an increase in surface roughness results in an increase in slope of the correlation line for each tube. The question whether to correlate the data on the film or surface basis cannot be resolved by comparison of the data scatter in figures 6 and 7. Essential to the resolution of this question is a knowledge of the correct variation of thermal conductivity of air with temperature, which has not been firmly established experimentally.

Modified correlation based on film temperature and friction velocity. - In figures 6 and 7, it was shown that, although the modified surface and the modified film methods of plotting both resulted in a good correlation of the heat-transfer data for each of the tubes investigated, neither method enabled correlation of the data for all degrees of roughness. This was to be expected inasmuch as no measure of surface roughness was included in the correlation parameters. If use were made of a parameter that includes the friction coefficient, which is a final measure of over-all surface roughness, correlation of the heat-transfer data for all the tubes investigated might be expected. A parameter that involves friction coefficient is the Reynolds number employing friction velocity  $\frac{\rho V_T D}{\mu}$  where  $V_T$  is given by  $V \sqrt{\frac{f}{2}}$ .

The possibility of using the friction velocity  $V_\tau$  in place of the bulk velocity  $V_b$  in the Reynolds number used in correlating heat-transfer data for rough tubes is also indicated in reference 13; these data were obtained for water flowing through artificially roughened brass pipes having various degrees of pyramidal-shaped roughness. Further verification of the friction velocity dependency, as applied to the experimental data of reference 13, is indicated by theory in reference 14.

Both the modified film and modified surface heat-transfer correlations were considered for use with the friction velocity; however, use of the film temperature results in the best correlation of the data for all tubes. Accordingly, the modified film correlation parameters of figure 7 were again used with the exception that the air bulk velocity  $V_b$  in the Reynolds number was replaced by the friction velocity  $V_\tau$

(taken as  $V_b \sqrt{\frac{f_f}{2}}$ ), which is more generally defined as the square root of the ratio of the shear stress at the wall to the fluid mass density (or  $\sqrt{\frac{\tau_w}{\rho}}$ ).

Average heat-transfer coefficients for all the tubes investigated herein, when plotted in this manner, are shown in figure 8, where  $(hD/k_f)/(c_{p,f}\mu_f/k_f)^{0.4}$  is plotted against  $\rho_f V_\tau D/\mu_f$ . Despite the wide variation in surface roughness represented herein, the heat-transfer data for all tubes can be fairly well represented by a mean line (solid) having the equation, above a value of  $\rho_f V_\tau D/\mu_f$  of 600,

$$\frac{hD}{k_f} = 0.040 \left( \frac{\rho_f V_\tau D}{\mu_f} \right)^{1.0} \left( \frac{c_{p,f} \mu_f}{k_f} \right)^{0.4} \quad (13)$$

The slope of the line best representing the data is 0.99; for convenience, however, a value of 1.0 is used. The maximum scatter for all the data is less than  $\pm 15$  percent as compared with  $\pm 26$  percent for the modified surface correlation of figure 6(b) if a mean line were drawn through all the data.

#### Friction Data With No Heat Addition

Comparison of friction coefficients. - A comparison of the average isothermal friction coefficients obtained herein for the smooth tube and rough tubes A, B, and C is presented in figure 9, where  $f_b/2$  is plotted against  $DG/\mu_b$ . Also included is the Blasius line (solid) representing the relation between friction coefficient and Reynolds number for turbulent flow in smooth tubes, which is

$$\frac{f_b}{2} = 0.0395 \left( \frac{DG}{\mu_b} \right)^{-0.25} \quad (14)$$

and the line (dashed) representing the friction coefficient relation in the laminar flow region, which is

$$\frac{f_b}{2} = 8.0 \left( \frac{DG}{\mu_b} \right)^{-1.0} \quad (15)$$

The data for the smooth tube show good agreement with the Blasius line in the turbulent flow region. The data for rough tubes A, B, and C, however, break away from the Blasius line and follow patterns somewhat similar to that obtained for the Nikuradse sand-grain rough-tube experiments of reference 6. That is, the friction coefficients for a given roughness break away from the Blasius line at some value of Reynolds number, which decreases with increase in surface roughness, and then follow a horizontal line (that is, independent of Reynolds number) appropriate to that degree of roughness. For any such curve, as interpreted by Nikuradse and others, the horizontal portion represents a region of complete turbulence, while the curved portion, bounded by the Blasius line and the point at which complete turbulence begins, represents a region of incomplete turbulence. This interpretation of complete and incomplete turbulence will also be used herein.

The effect of surface roughness on friction coefficients may be examined, in somewhat more detail, in the regions of complete turbulence, incomplete turbulence, and laminar flow. In the complete turbulence region, the friction coefficient for each tube is a constant (independent of Reynolds number); the value of the constant depends only on the overall degree of roughness, as influenced by the pertinent geometric factors. It is noteworthy, then, that the constant value of friction coefficient for tube A is higher than that for tube B, since tube B has a higher value of conventional roughness ratio than tube A; hence, it may be concluded that the conventional roughness ratio is not an adequate measure of relative roughness for completely turbulent flow in square-thread passages.

In the region of incomplete turbulence, the conventional roughness ratio, although not the sole measure of roughness, may be expected to be influential inasmuch as the effect of a projection depends on its height relative to the height of the laminar boundary layer. Hence, the incomplete turbulence region may be expected to prevail over a decreasing Reynolds number range as the conventional roughness ratio increases. This is borne out by the data. For example, tube C shows incomplete turbulence over a Reynolds number range from 3000 to about 100,000; tube A, from 3000 to about 40,000; and tube B, from 3000 to about

25,000. Further, tube B, having the highest value of conventional roughness ratio, shows the highest friction coefficient in this region.

In the laminar flow region (Reynolds numbers  $\leq 2000$ ) the effect of surface roughness is negligible inasmuch as the friction coefficient for tube A is in good agreement with the laminar flow line for smooth pipes, as are the data for all the tubes investigated herein within the accuracy of the data in this region. The small effect of roughness in the low Reynolds number region is further indicated by the heat-transfer data (fig. 6(b)), which showed no effect of roughness for modified surface Reynolds numbers less than 3000.

Comparison of surface roughness. - For the Nikuradse sand-grain rough-tube data of reference 6, von Karman has shown that in the complete turbulence region the constant value of friction coefficient  $f_c$  is dependent only upon the roughness ratio  $e/r$ . Inasmuch as the heat-transfer data and the friction data with no heat addition suggest that the conventional roughness ratio is not an adequate measure of roughness for a square-thread-type element in the complete turbulence range, the physical dimension of the square-thread elements for rough tubes A, B, and C were examined to evaluate their influence on the friction coefficient  $f_c$ . The physical dimensions of the square-thread elements for rough tubes A, B, and C are tabulated in table I with ratios of thread height to thread width  $e/w$ , thread space (distance between threads) to thread width  $s/w$ , and the conventional roughness ratio  $e/r$ ; the measured value of  $f_c$  is also included.

TABLE I - COMPARISON OF SQUARE-THREAD ELEMENTS FOR  
ROUGH TUBES A, B, and C INVESTIGATED HEREIN

Rough tube	$e/w$	$s/w$	$e/r$	$f_c$
A	1.37	1.00	0.025	0.0122
B	1.12	1.30	.037	.0106
C	0.88	1.00	.016	.0058

In order to isolate the effect of each of these variables on the friction coefficient  $f_c$ , the rough tubes used herein were compared with those of reference 15 for tubes having similar square-thread-type roughnesses. Accordingly, the physical dimensions for the tubes of reference 15 are tabulated in table II.

TABLE II - COMPARISON OF SQUARE-THREAD ELEMENTS FOR  
ROUGH TUBES USED IN REFERENCE 15

Rough tube	e/w	s/w	e/r	$f_c$
I <sub>S</sub>	0.934	1.033	0.0111	0.00592
I <sub>m</sub>	0.928	1.018	0.0219	0.00630
I <sub>l</sub>	0.929	1.020	0.0390	0.00630
II	0.928	3.02	0.0219	0.0169
III	0.928	7.06	0.0219	0.0238

A comparison of the values of  $f_c$  obtained for rough tubes I<sub>S</sub>, I<sub>m</sub>, and I<sub>l</sub> (table II), for which a nearly fourfold increase in e/r resulted in less than 10 percent increase in  $f_c$ , would indicate that the friction coefficient in the complete turbulence region is essentially independent of the conventional roughness ratio e/r (the values of e/w and s/w are practically constant).

The effect of s/w on the friction coefficient  $f_c$  is shown in figure 10, where  $f_c$  is plotted against s/w for rough tubes I<sub>m</sub>, II, and III with each tube represented by a single point. The effects of e/w and e/r are not involved in this plot since these values are constant from tube to tube (table II). The s/w effect is best represented (fig. 10) for these tubes by a line (solid) having an equation of the form

$$f_c = C(s/w)^{0.80} \quad (16)$$

The effect of e/w on the friction coefficient  $f_c$  is shown in figure 11, where  $f_c$  is plotted against e/w for rough tubes A, B, and C; the points representing tubes I<sub>S</sub>, I<sub>m</sub>, and I<sub>l</sub> are also included. Tubes A and C (table I) have s/w values of 1.00 while that for tube B is 1.30; hence, the  $f_c$  value for tube B was corrected (fig. 11) to a s/w value of 1.00 by use of the data of figure 10. As a result, the effects of s/w and e/r are not involved in figure 11, as the s/w values are effectively constant (1.00) and the e/r effect is not involved (as previously pointed out). The e/w effect is best represented by a line (solid) having an equation of the form

$$f_c = C(e/w)^{1.70} \quad (17)$$

The  $s/w$  and  $e/w$  effects (equations (16) and (17), respectively) were then combined into an equation of the form

$$f_c = C(s/w)^{0.80}(e/w)^{1.70} \quad (18)$$

or

$$C = \frac{f_c}{(s/w)^{0.80}(e/w)^{1.70}} \quad (19)$$

The constant  $C$  in equation (19) was evaluated for each tube used herein as well as for those of reference 15. The values of  $C$  are plotted against the corresponding values of  $e/r$  in figure 12, which shows (as previously indicated in table II) that the friction coefficient  $f_c$  is independent of the conventional roughness ratio. The horizontal line which best represents the data for all the square-thread tubes considered has an ordinate value of 0.0068 where the maximum scatter of the data is  $\pm 16$  percent; or, in equation (18),

$$f_c = 0.0068(s/w)^{0.80}(e/w)^{1.70} \quad (20)$$

The value of  $C$  best representing the data for rough tubes A, B, and C is 0.0072. This equation, which permits estimation of the friction coefficient in the complete turbulence region, is valid only for this region; this point is better illustrated in a subsequent figure.

Equation (20) is also purely empirical and is based on data for threaded tubes having ranges of  $e/w$  from 0.88 to 1.37,  $s/w$  from 1.00 to 7.06, and  $e/r$  from 0.011 to 0.039 (fig. 12) and should be used with discretion in extrapolating to values outside these ranges.

#### Friction Data With Heat Addition

Conventional correlation based on bulk temperature. - The average friction coefficients obtained herein for the smooth tube with heat addition are presented in the conventional manner in figure 13(a), where  $f_b/2$  is plotted against  $DG/\mu_b$ . Included for comparison are the data for no heat addition and the lines representing the Blasius and laminar-flow relations.

Data obtained at the lowest surface temperature level (that is,  $T_s = 885^\circ \text{R}$ ) show fair agreement with those for no heat addition. With an increase in  $T_s/T_b$ , however, the friction coefficients progressively decrease at the higher Reynolds numbers and increase at the lower

Reynolds numbers. Similar results were obtained for the smooth-tube investigation of references 1, 4, and 5.

The data for rough tubes A, B, and C, when plotted in this manner, resulted in a  $T_s/T_b$  effect similar to that obtained for the smooth tube. In the case of rough tube A (fig. 13(b)), having the highest degree of surface roughness investigated herein, the actual  $T_s/T_b$  effect is more clearly shown in the complete turbulence region where the friction coefficient is independent of Reynolds number. The data for rough tubes B and C (not shown), having a decreasing order of surface roughness, gave results intermediate to those for rough tube A and the smooth tube.

Modified correlation based on film temperature. - Modified film friction coefficients for the smooth tube with heat addition are presented in figure 14(a), where  $f_f/2$  is plotted against  $\rho_f V_b D / \mu_f$ , the modified film Reynolds number. The film friction coefficient  $f_f$  was defined in equation (8). Included in figure 14(a) are the data for no heat addition and the lines representing the laminar flow and Blasius relations.

This method of plotting results in a fair correlation of the friction data for all temperature levels although there is some over-correction of the  $T_s/T_b$  effect at the lower Reynolds numbers.

The friction data for rough tubes A, B, and C, plotted in the same manner, are presented in figures 14(b), 14(c), and 14(d), respectively, which is the order of decreasing surface roughness. Similar results are obtained in each case with the data being fairly well correlated by this method of plotting, particularly at the higher Reynolds numbers. For each of the tubes investigated, however, the data follow a curve characteristic to that particular degree of surface roughness as previously pointed out for the isothermal data.

Modified correlation using roughness parameters. - In order to correlate the friction data for all the rough tubes investigated herein, the following method of plotting was employed: In figures 14(b), 14(c), and 14(d), it was shown that the effect of tube wall-to-bulk temperature ratio can be eliminated (particularly at the higher Reynolds numbers) for each of the rough tubes by use of the modified correlation based on film temperature. Moreover, a comparison of the surface roughness for the tubes used herein (together with those of reference 15) indicated (fig. 12) that the friction coefficient in the complete turbulence region  $f_c$  can be predicted by an equation of the form

$$f_c = C(s/w)^{0.80} (e/w)^{1.70} \quad (21)$$

where  $C$  has a value of 0.0072 for the tubes used herein (0.0068 for all the tubes considered).

Hence, the friction data for rough tubes A, B, and C are presented in figure 15, where  $\frac{f_f}{2} / (s/w)^{0.80} (e/w)^{1.70}$  is plotted against the modified film Reynolds number. Inasmuch as equation (21) is directly applicable only in the complete turbulence region, the data of figure 15 are restricted to values of Reynolds number greater than 20,000; this region was seen in figure 9 to fully represent the complete turbulence region for rough tubes A and B. For rough tube C complete turbulence was not attained until Reynolds numbers considerably greater than 20,000 were reached, which is reflected in figure 15.

The friction data (both with and without heat addition) for all the rough tubes (fig. 15) are in good agreement in the complete turbulence region. The greater part of the data separation at the lower Reynolds numbers results from the data of tube C being considerably below the complete turbulence region; the smaller separation in the case of tubes A and B stems from the  $T_s/T_b$  effect, as pointed out in figure 14. The equation of the line representing the friction data for all tubes in the complete turbulence region is

$$f_f/2 = 0.0036(s/w)^{0.80}(e/w)^{1.70} \quad (22)$$

#### SUMMARY OF RESULTS

An investigation of heat transfer and friction was conducted with air flowing through electrically heated Inconel tubes having various degrees of square-thread-type roughness, an inside diameter of 1/2 inch, and a length of 24 inches. Data were obtained for threaded tubes having conventional roughness ratios (height of thread/radius of tube) of 0 (smooth tube), 0.016, 0.025, and 0.037 over a range of bulk Reynolds numbers up to 350,000, average inside-tube-wall temperatures up to 1950° R, and heat-flux densities up to 115,000 Btu per hour per square foot. The results of this investigation are as follows:

1. The experimental data showed that both heat transfer and friction increased with increase in surface roughness, becoming more pronounced with increase in Reynolds number; for a given roughness, both heat transfer and friction were also influenced by the tube wall-to-bulk temperature ratio.

2. A satisfactory correlation of the heat-transfer data for all the tubes investigated was obtained by use of a modification of the conventional Nusselt correlation parameters wherein the mass velocity  $G$  (or product of average air density and velocity evaluated at the bulk temperature,  $\rho_b V_b$ ) in the Reynolds number was replaced by the product

of air density evaluated at the average film temperature and the friction velocity,  $\rho_f V_\tau$ ; in addition, the physical properties of air were evaluated at the average film temperature.

3. The isothermal friction data for the rough tubes, when plotted in the conventional manner, resulted in curves similar to those obtained by other investigators. That is, the friction coefficients for a given roughness break away from the Blasius line (representing turbulent flow in smooth tubes) at some value of Reynolds number, which decreases with increase in surface roughness, and then follow a horizontal line (that is, independent of Reynolds number). A further comparison of the friction data indicated that the conventional roughness ratio is not an adequate measure of relative roughness for tubes having a square-thread-type element.

4. A fair correlation of the friction data with heat addition was obtained, for each of the tubes investigated, by use of a modified correlation wherein the friction coefficient based on average film density was plotted against the modified film Reynolds number; however, the data for each tube retained the curve characteristic of that particular roughness. A good correlation of the friction data for all the rough tubes was obtained for the complete turbulence region by incorporating a roughness parameter in the modified film correlation. No correlation was obtained for the region of incomplete turbulence.

Lewis Flight Propulsion Laboratory  
National Advisory Committee for Aeronautics  
Cleveland, Ohio

## APPENDIX - SYMBOLS

The following symbols are used in this report:

C	constant
$c_p$	specific heat of air at constant pressure, Btu/(lb)(°F)
D	inside diameter of test section, ft
f	average friction coefficient
$f_b$	average bulk friction coefficient
$f_c$	average bulk friction coefficient (complete turbulence region)
$f_f$	modified film friction coefficient
G	mass velocity (mass flow per unit cross-sectional area), lb/(hr)(sq ft)
g	acceleration due to gravity, $4.17 \times 10^8$ ft/hr <sup>2</sup>
h	average heat-transfer coefficient, Btu/(hr)(sq ft)(°F)
k	thermal conductivity of air, Btu/(hr)(sq ft)(°F/ft)
$k_t$	thermal conductivity of Inconel, Btu/(hr)(sq ft)(°F/ft)
L	effective heat-transfer length of test section, ft
p	static pressure, lb/sq ft abs
$\Delta p$	over-all static-pressure drop across test section, lb/sq ft
$\Delta p_{fr}$	friction static-pressure drop across test section, lb/sq ft
Q	rate of heat transfer to air, Btu/hr
R	gas constant for air, 53.35 ft-lb/(lb)(°F)
r	inside radius of test section, ft
S	heat-transfer area of test section, sq ft
T	total temperature, °R
$T_b$	average bulk temperature equal to average of entrance and exit total temperatures, °R

$T_f$	average film temperature equal to half the sum of average bulk and average inside-tube-wall temperatures, $^{\circ}\text{R}$
$T_s$	average inside-tube-wall temperature, $^{\circ}\text{R}$
$t$	static temperature, $^{\circ}\text{R}$
$V$	velocity, ft/hr
$V_{\tau}$	friction velocity, ft/hr $\left( V_{\tau} = \sqrt{\frac{\tau g}{\rho}} = V \sqrt{\frac{f}{2}} \right)$
$W$	air flow, lb/hr
$\mu$	absolute viscosity of air, lb/(hr)(ft)
$\rho$	density of air, lb/cu ft
$\rho_{av}$	average density of air, lb/cu ft
$\tau$	shear stress at wall, lb/sq ft

## Dimensionless parameters:

$hD/k$	Nusselt number
$c_p\mu/k$	Prandtl number
$DG/\mu$	Reynolds number
$\rho_f V_b D/\mu_f$	modified film Reynolds number
$\rho_f V_{\tau} D/\mu_f$	modified film Reynolds number with friction velocity
$\rho_s V_b D/\mu_s$	modified surface Reynolds number

## Roughness characteristics:

$e/r$	conventional roughness ratio
$e/w$	ratio of thread height to thread width
$s/w$	ratio of thread space to thread width

where

e	height of roughness element (thread height), ft	} except as noted in figure 3
s	thread space (distance between threads), ft	
w	thread width, ft	

## Subscripts:

- 1 test-section entrance
- 2 test-section exit
- i inner surface of test section
- o outer surface of test section
- b bulk (when applied to properties, indicates evaluation at average bulk temperature)
- f film (when applied to properties, indicates evaluation at average film temperature)
- s surface (when applied to properties, indicates evaluation at average inside-tube-wall temperature)

## REFERENCES

1. Lowdermilk, Warren H., and Grele, Milton D.: Heat Transfer from High-Temperature Surfaces to Fluids. II - Correlation of Heat-Transfer and Friction Data for Air Flowing in Inconel Tube with Rounded Entrance. NACA RM E8L03, 1949.
2. Sams, Eldon W., and Desmon, Leland G.: Heat Transfer from High-Temperature Surfaces to Fluids. III - Correlation of Heat-Transfer Data for Air Flowing in Silicon Carbide Tube with Rounded Entrance, Inside Diameter of 3/4 Inch, and Effective Length of 12 Inches. NACA RM E9D12, 1949.
3. Desmon, Leland G., and Sams, Eldon W.: Correlation of Forced-Convection Heat-Transfer Data for Air Flowing in Smooth Platinum Tube with Long-Approach Entrance at High Surface and Inlet-Air Temperatures. NACA RM E50H23, 1950.

4. Lowdermilk, Warren H., and Grele, Milton D.: Influence of Tube-Entrance Configuration on Average Heat-Transfer Coefficients and Friction Factors for Air Flowing in an Inconel Tube. NACA RM E50E23, 1950.
5. Humble, Leroy V., Lowdermilk, Warren H., and Desmon, Leland G.: Measurements of Average Heat-Transfer and Friction Coefficients for Subsonic Flow of Air in Smooth Tubes at High Surface and Fluid Temperatures. NACA Rep. 1020, 1951.
6. Nikuradse, J.: Strömungsgesetze in Rauhen Rohren. V.D.I. Forschungsheft 361 (Berlin), 1933.
7. Rouse, Hunter: Evaluation of Boundary Roughness. Proc. Second Hydraulic Conference, Bull. 27, Univ. of Iowa, 1943, pp. 105-116.
8. Tribus, Myron, and Boelter, L. M. K.: An Investigation of Aircraft Heaters. II - Properties of Gases. NACA ARR, Oct. 1942.
9. Keenan, Joseph H., and Kaye, Joseph: Gas Tables. John Wiley & Sons, Inc., 1948.
10. Bernardo, Everett, and Eian, Carroll S.: Heat-Transfer Tests of Aqueous Ethylene Glycol Solutions in a Electrically Heated Tube. NACA ARR E5F07, 1945.
11. McAdams, William H.: Heat Transmission. McGraw-Hill Book Co., Inc., 2d ed., 1942, p. 168.
12. Deissler, Robert G.: Analytical Investigation of Turbulent Flow in Smooth Tubes with Heat Transfer with Variable Fluid Properties for a Prandtl Number of 1. NACA TN 2242, 1950.
13. Cope, W. F.: The Friction and Heat Transmission Coefficients of Rough Pipes. Rep. 3903, British A.R.C., Feb. 21, 1939.
14. Martinelli, R. C.: Heat Transfer to Molten Metals. Trans. A.S.M.E., vol. 69, no. 8, Nov. 1947, pp. 947-959.
15. Chu, H., and Streeter, V. L.: Fluid Flow and Heat Transfer in Artificially Roughened Pipes. Proj. No. 4918, Illinois Inst. of Tech., Aug. 1, 1949.

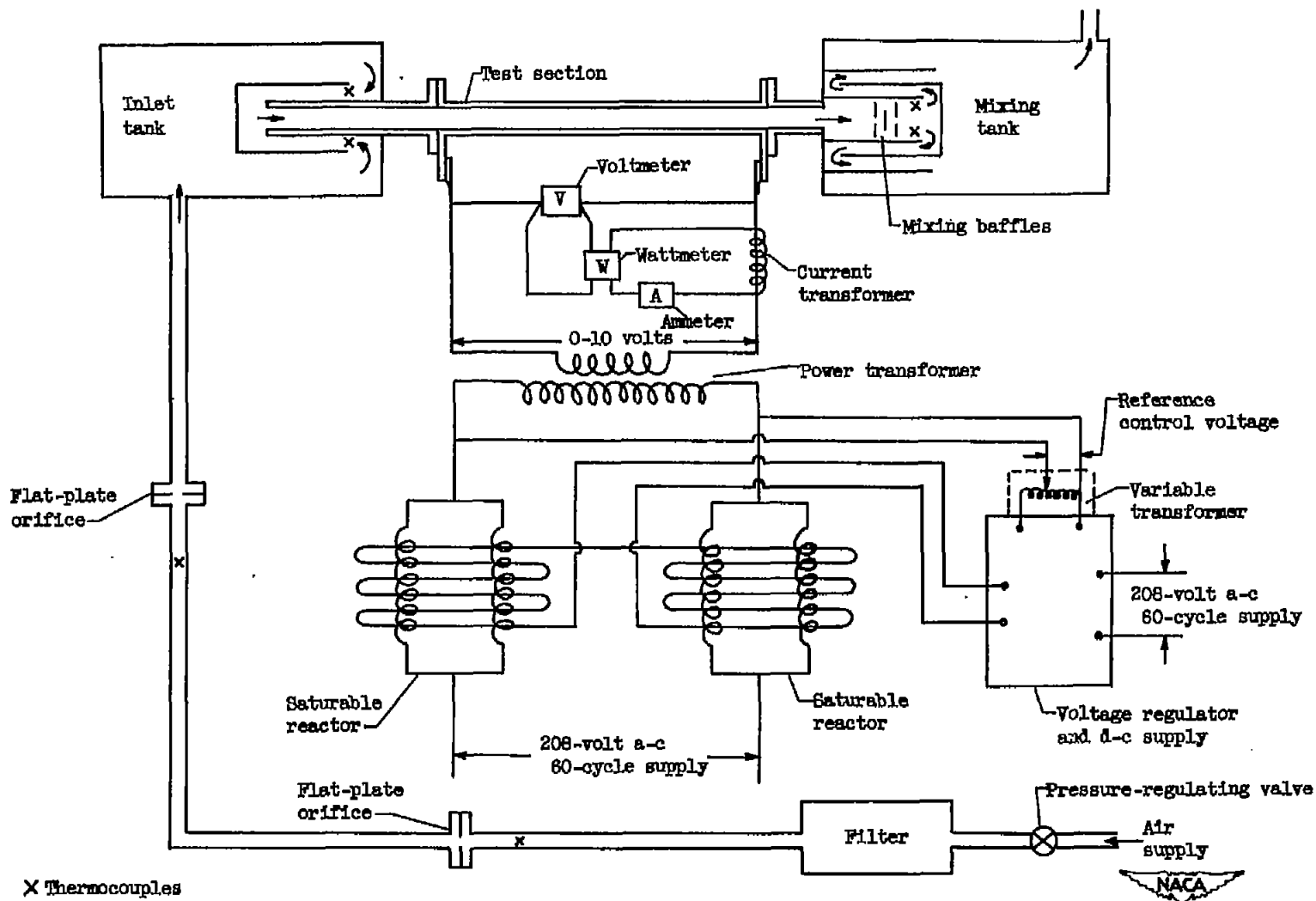


Figure 1. - Schematic diagram showing arrangement of experimental equipment.

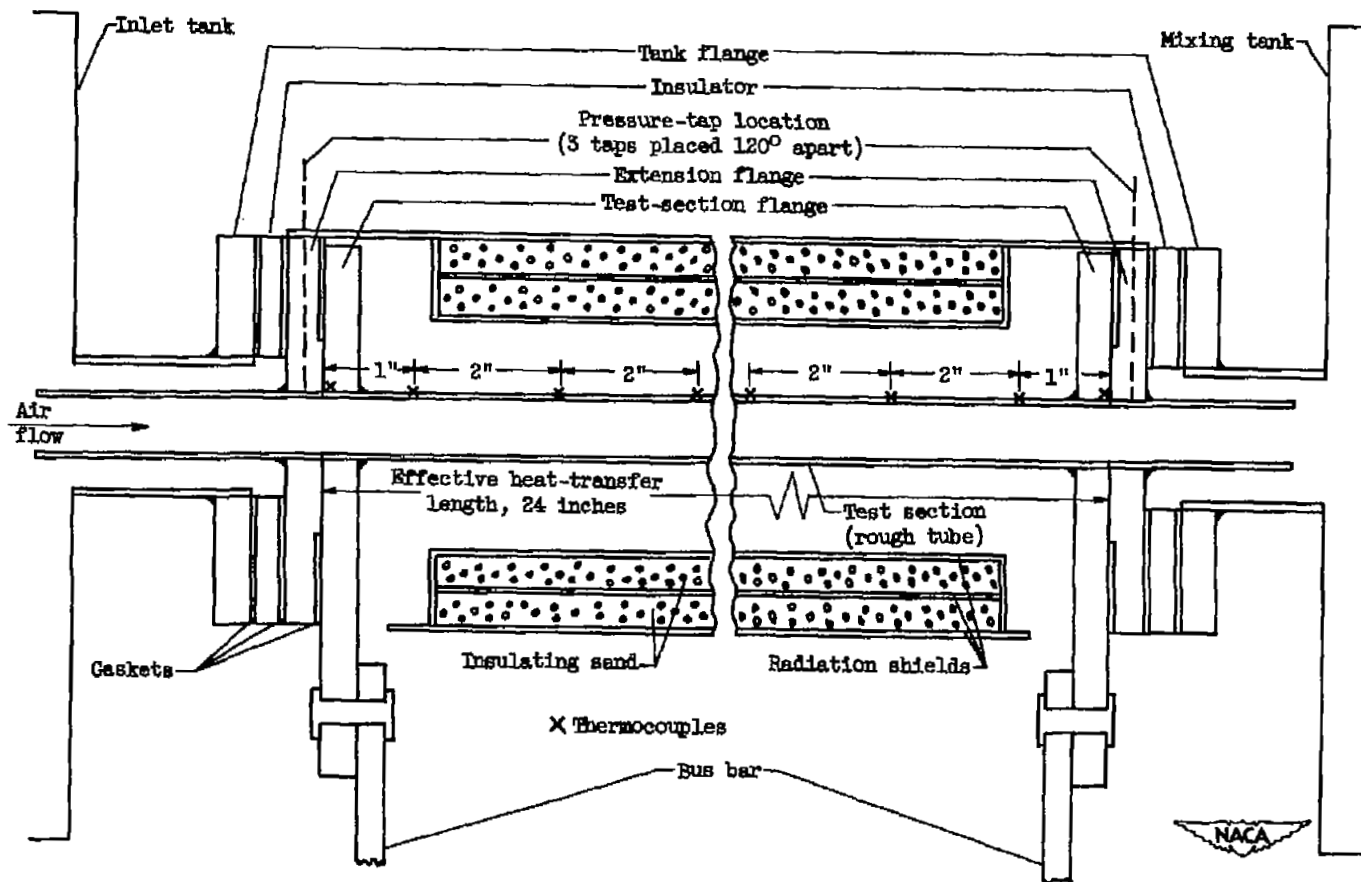
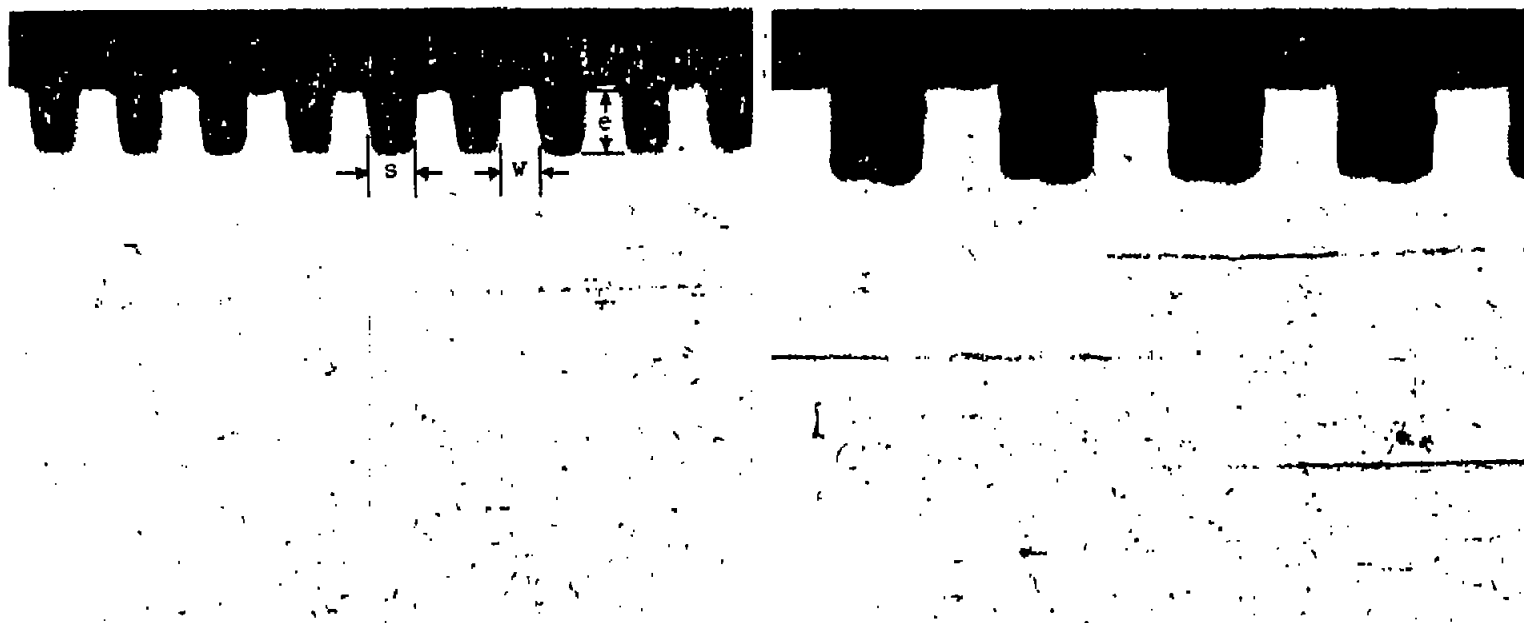


Figure 2. - Schematic diagram of typical test-section (rough tube) installation showing thermocouple and pressure-tap locations.



Tube A - nominal 0.005-inch square-thread tube.

Thread height (e) = 0.0065 inch  
 Thread width (w) = .0047 inch  
 Thread space (s) = .0047 inch

Tube B - nominal 0.010-inch square-thread tube.

Thread height (e) = 0.0095 inch  
 Thread width (w) = .0085 inch  
 Thread space (s) = .0110 inch

Tube C - honed version of tube A (no photograph).

Thread height (e) = 0.0042 inch  
 Thread width (w) = .0047 inch  
 Thread space (s) = .0047 inch

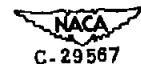


Figure 3. - Tube-wall cross-section photographs (150 magnification) of rough-tube samples showing roughness profiles or thread measurements or both.

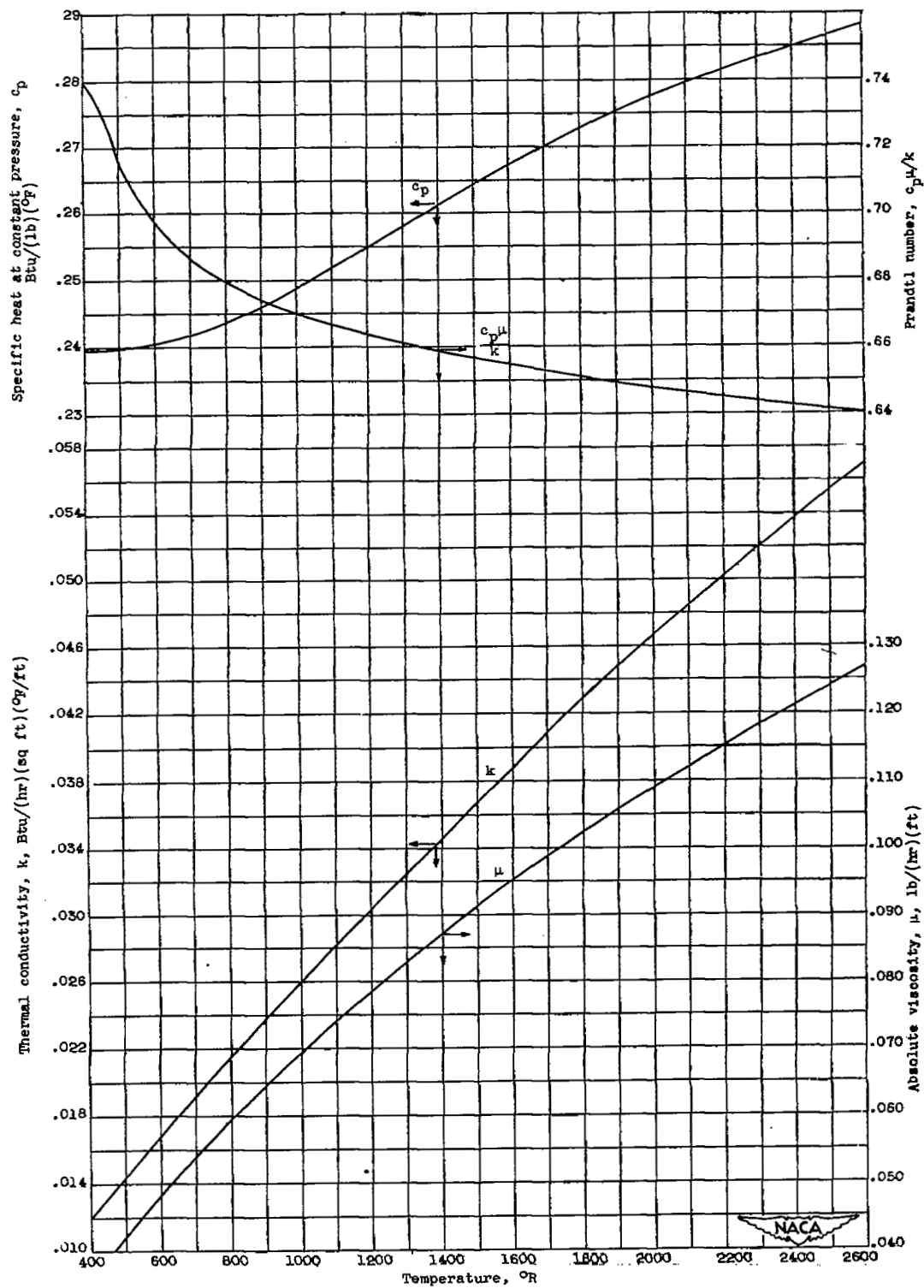
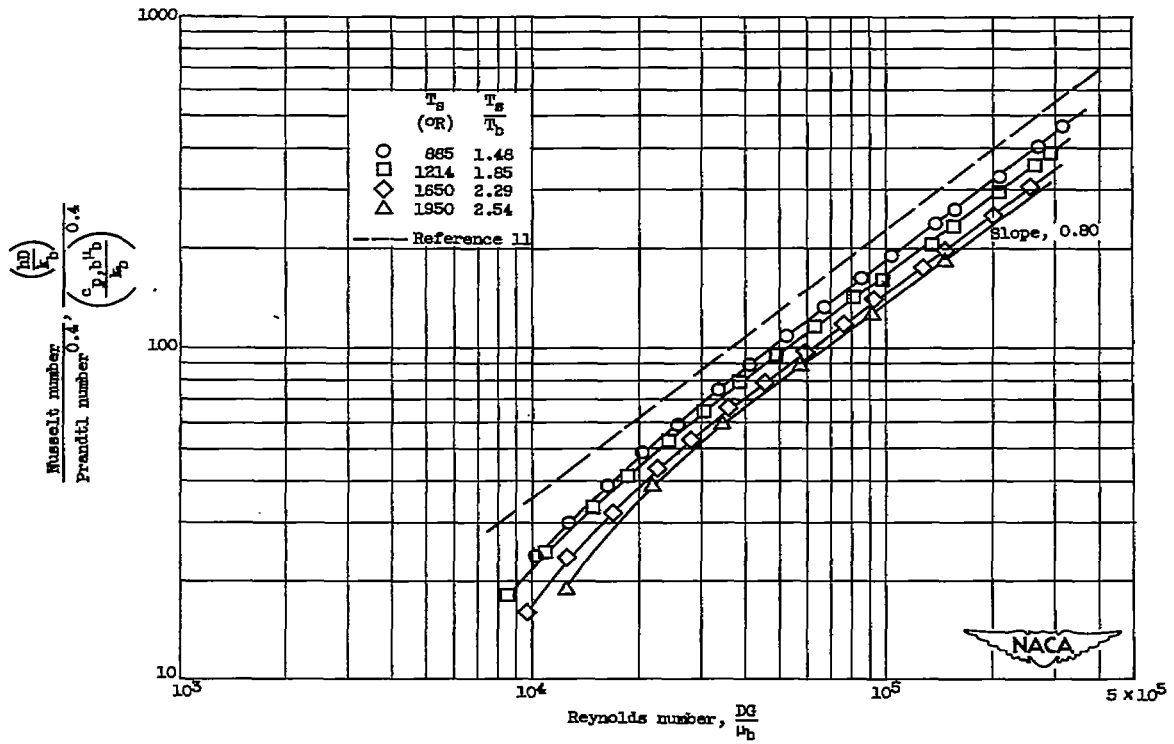
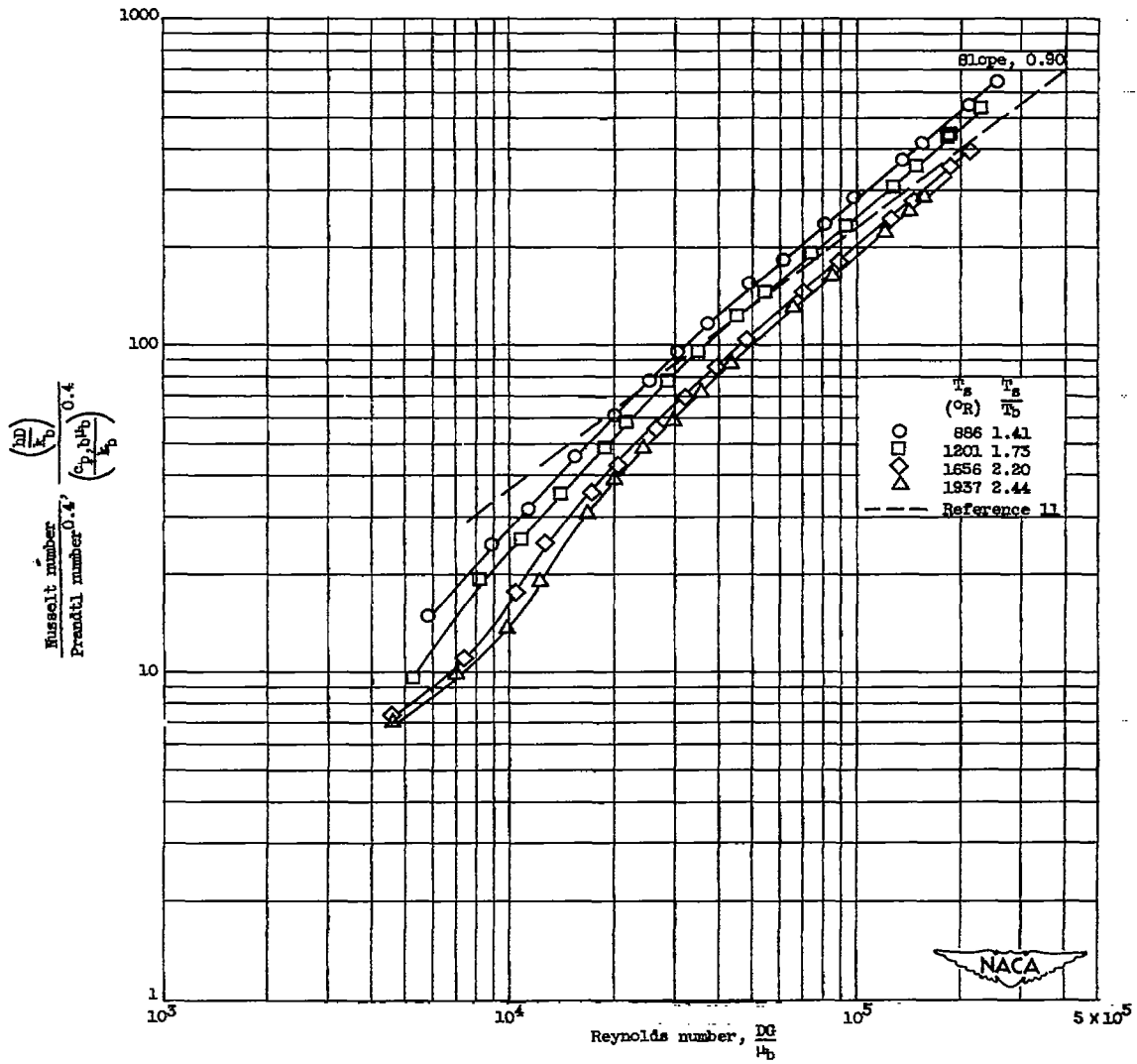


Figure 4. - Variation of specific heat at constant pressure, thermal conductivity, absolute viscosity, and Prandtl number of air with temperature. (Data from references 8 and 9.)



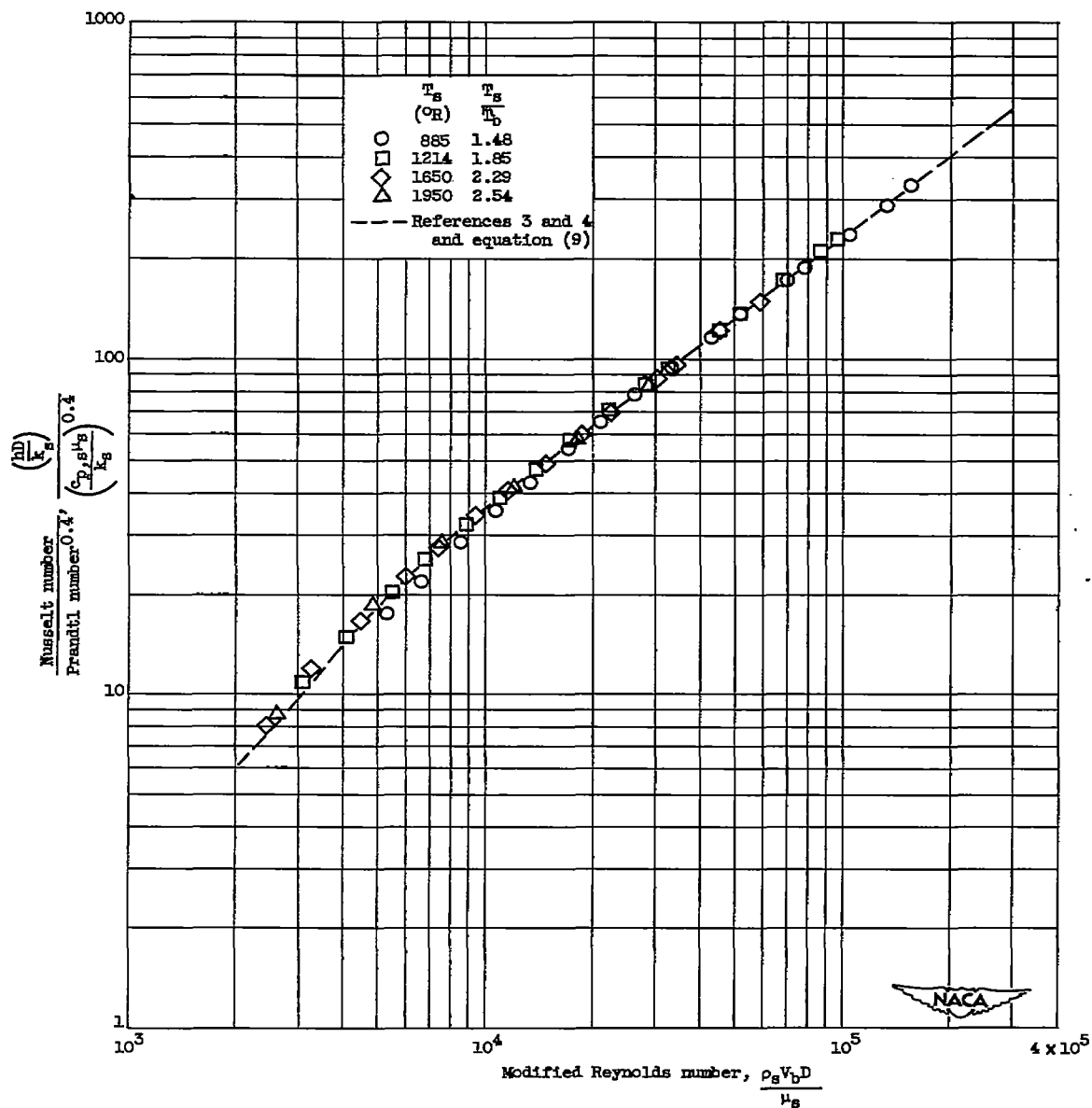
(a) Data for smooth tube. Conventional roughness ratio,  $e/r$ , 0.

Figure 5. - Conventional correlation of heat-transfer data. Physical properties of air evaluated at bulk temperature  $T_b$ .



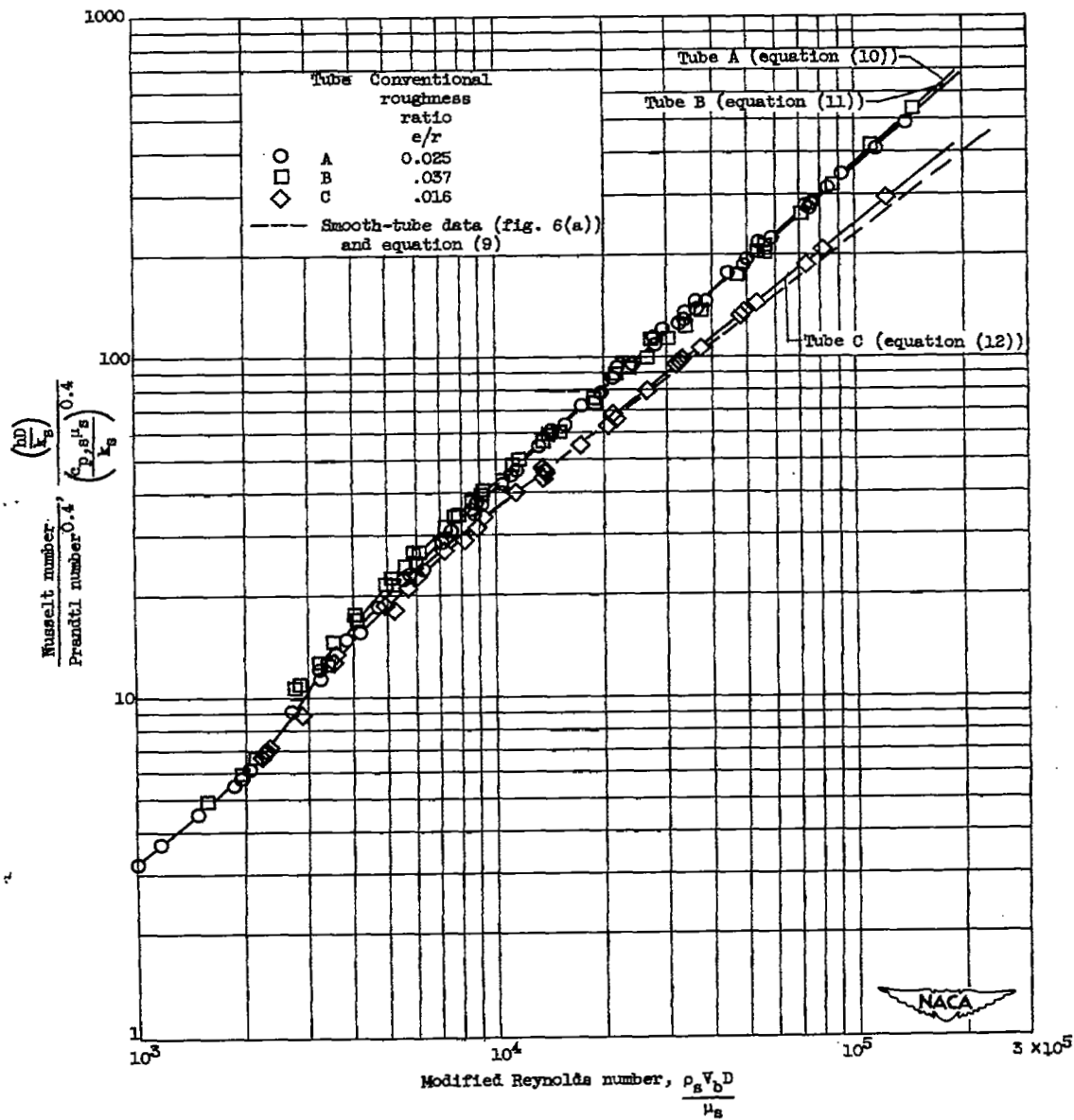
(b) Data for rough tube A. Conventional roughness ratio,  $e/r$ , 0.025.

Figure 5. - Concluded. Conventional correlation of heat-transfer data. Physical properties of air evaluated at bulk temperature  $T_b$ .



(a) Data for smooth tube. Conventional roughness ratio,  $e/r$ , 0.

Figure 6. - Correlation of heat-transfer data with modified surface Reynolds number. Physical properties of air evaluated at average surface temperature  $T_s$ .



(b) Data for rough tubes A, B, and C.

Figure 6. - Concluded. Correlation of heat-transfer data with modified surface Reynolds number. Physical properties of air evaluated at average surface temperature  $T_s$ .

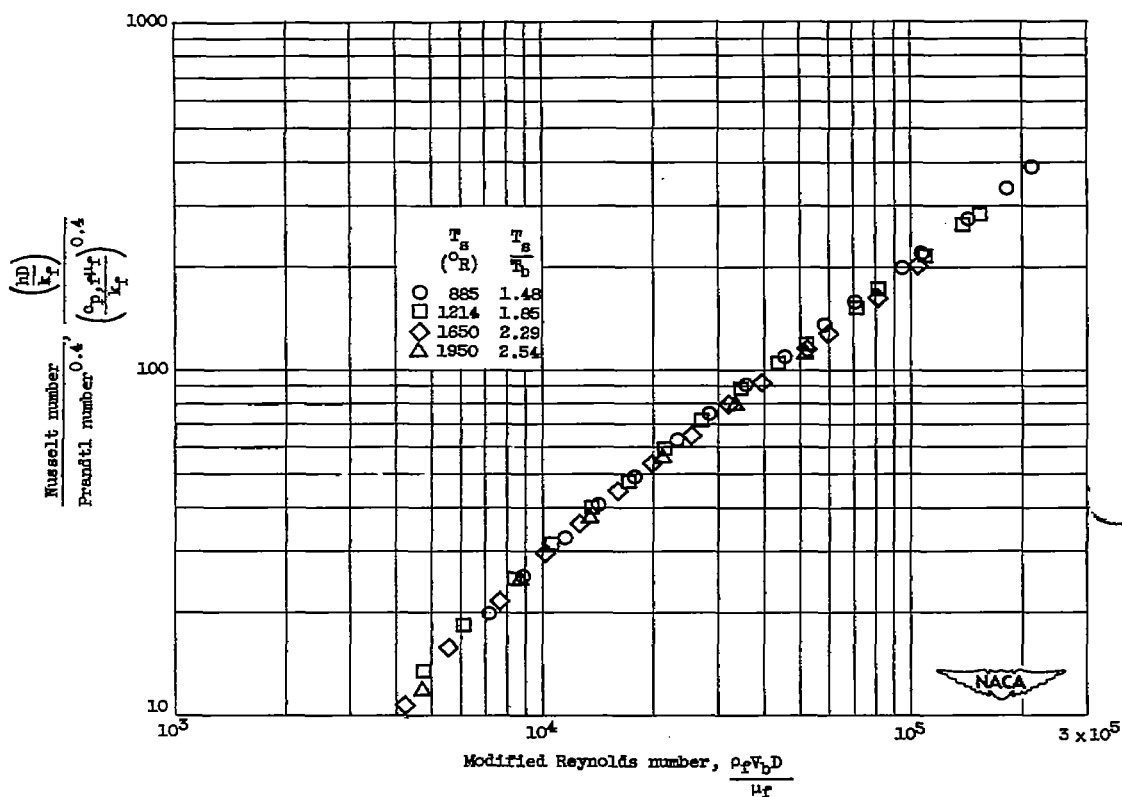


Figure 7. - Correlation of heat-transfer data for smooth tube (conventional roughness ratio, 0) with modified film Reynolds number. Physical properties of air evaluated at average film temperature  $T_f$ .

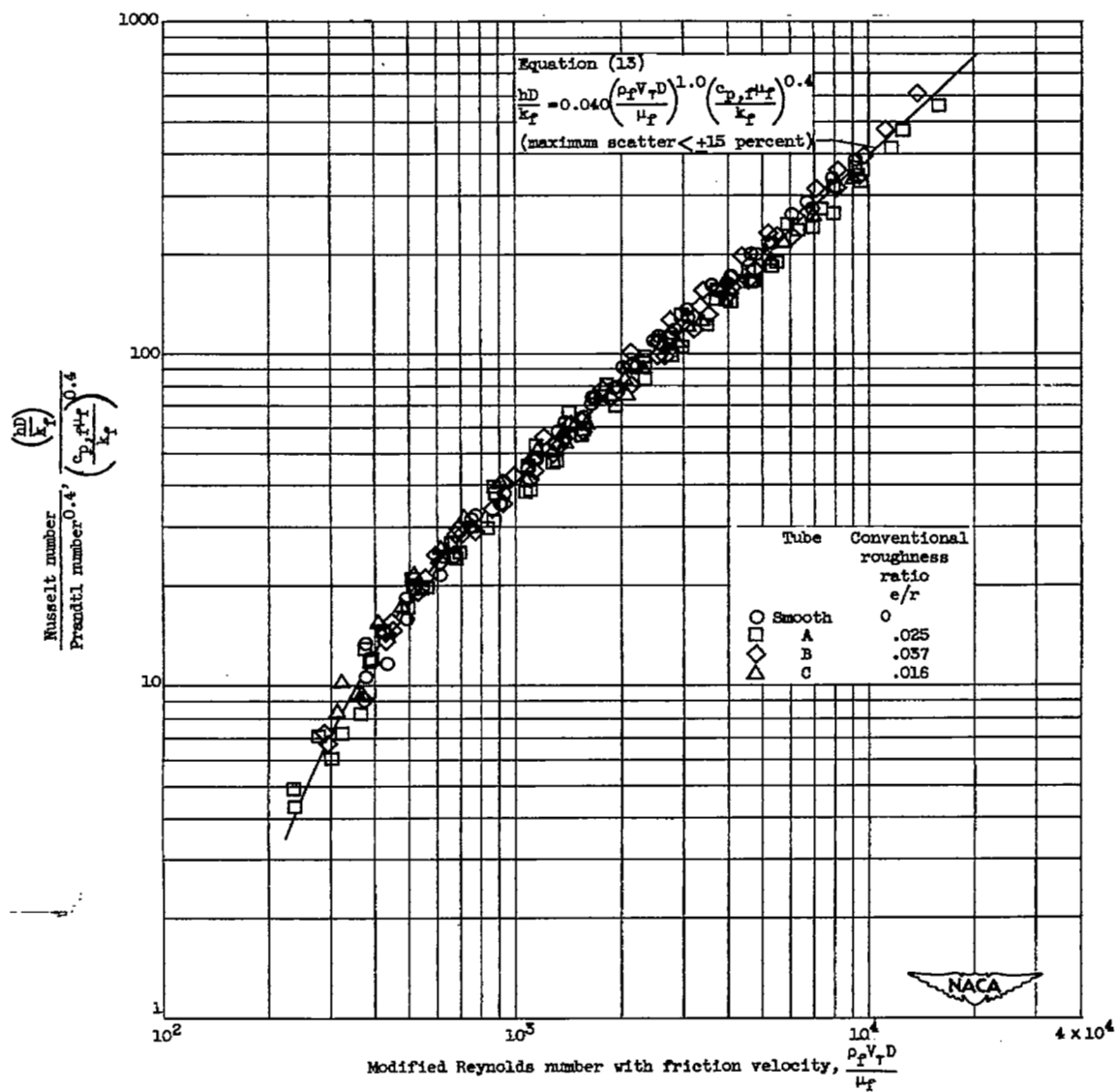


Figure 8. - Correlation of heat-transfer data with modified film Reynolds number and friction velocity. Physical properties of air evaluated at average film temperature  $T_f$ . Data for all tubes and temperature levels investigated.

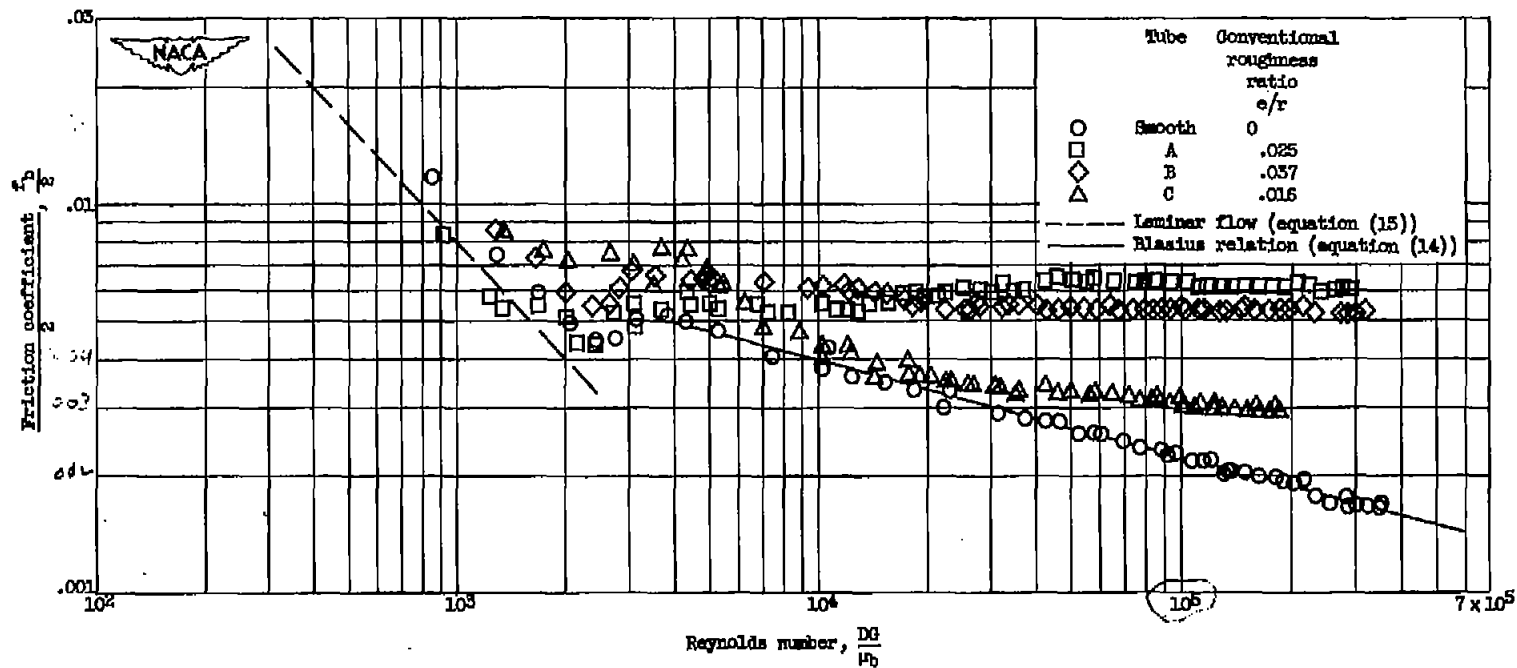


Figure 9. - Comparison of isothermal friction coefficients for smooth tube and rough tubes A, B, and C.

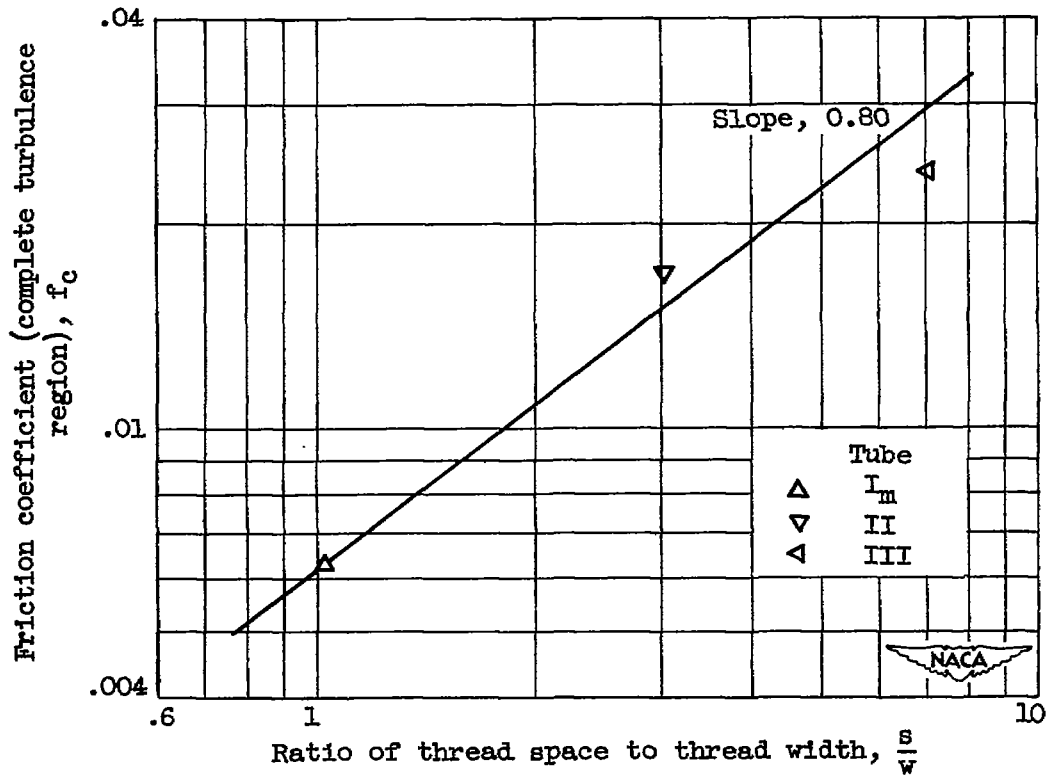


Figure 10. - Effect of ratio of thread space (distance between threads) to thread width on isothermal friction coefficients in complete turbulence region. Data for tubes I<sub>m</sub>, II, and III from reference 15.

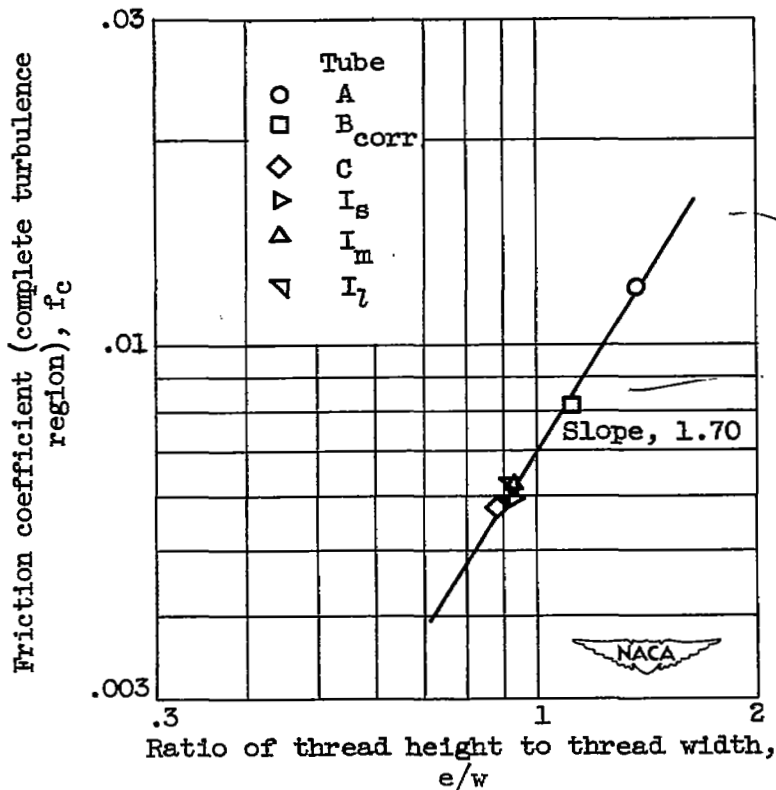


Figure 11. - Effect of ratio of thread height to thread width on isothermal friction coefficient in complete turbulence region. Data for rough tubes A, B, and C from present investigation and tubes I<sub>s</sub>, I<sub>m</sub>, and I<sub>t</sub> from reference 15.

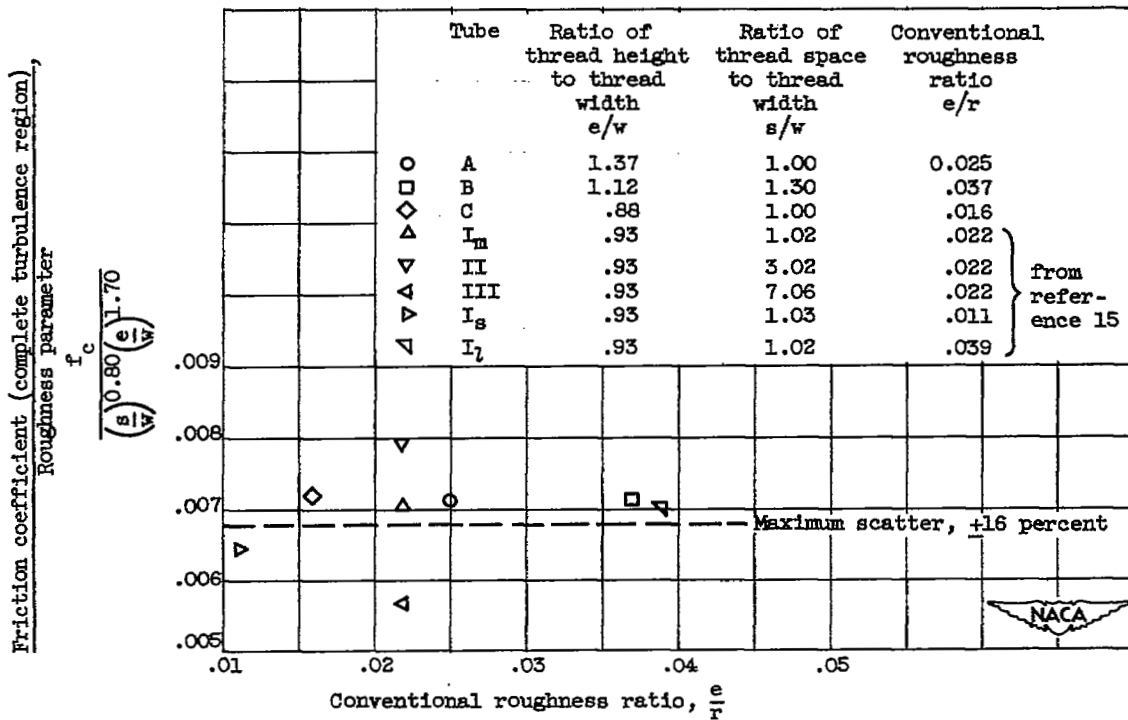
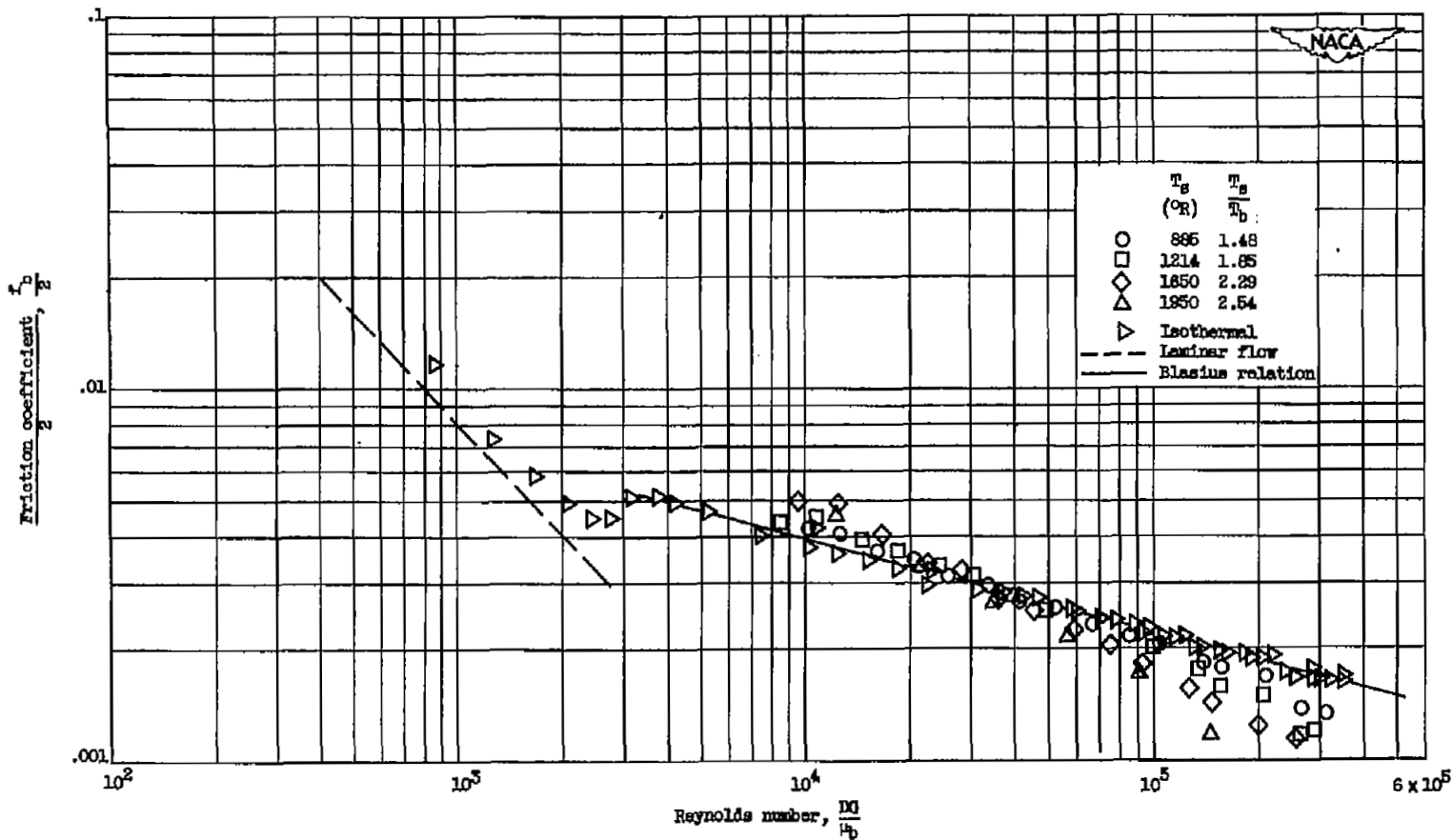
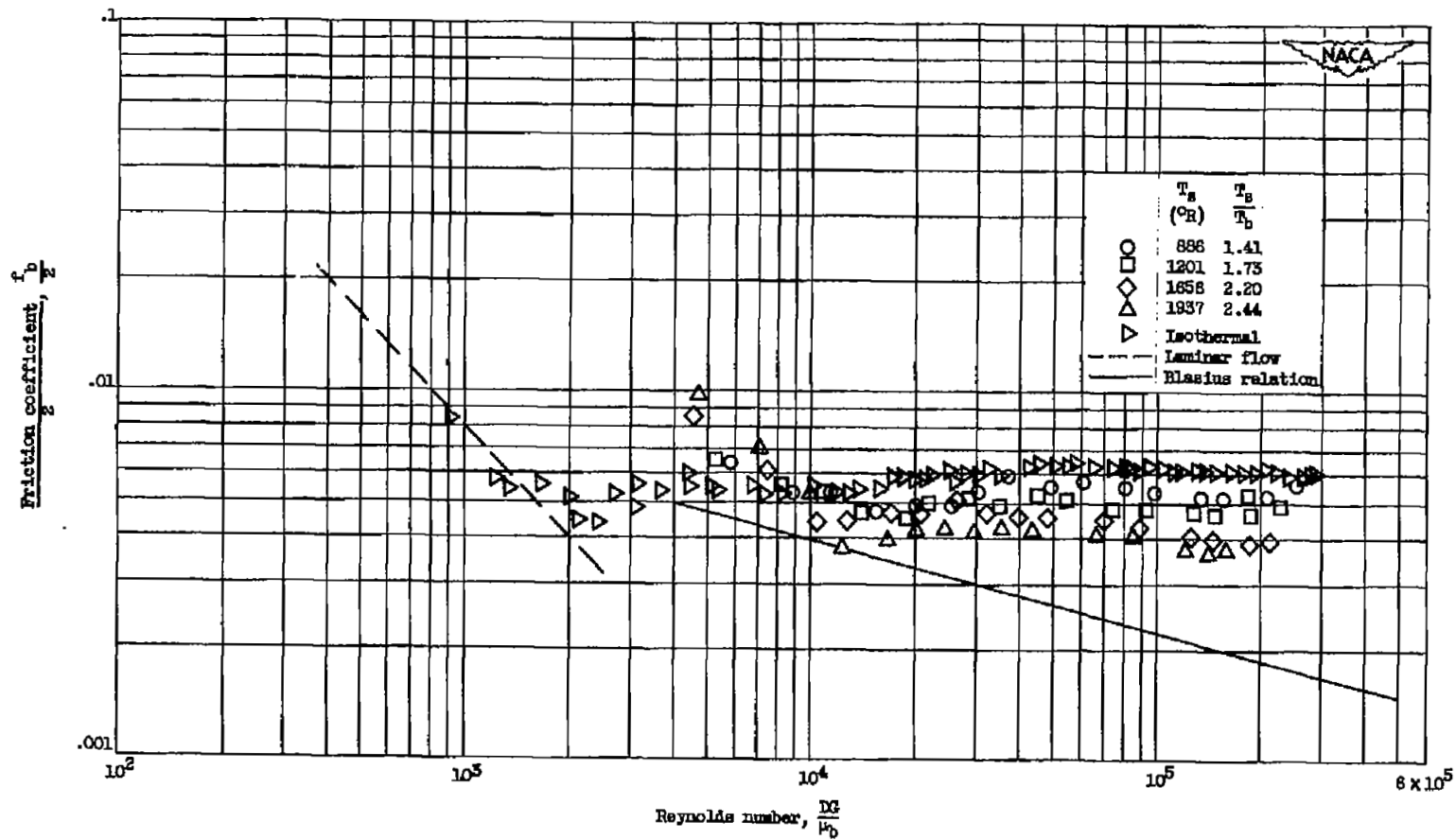


Figure 12. - Effect of conventional roughness ratio on friction parameter  $f_c/(s/w)^{0.80} (e/w)^{1.70}$  for isothermal data in complete turbulence region.



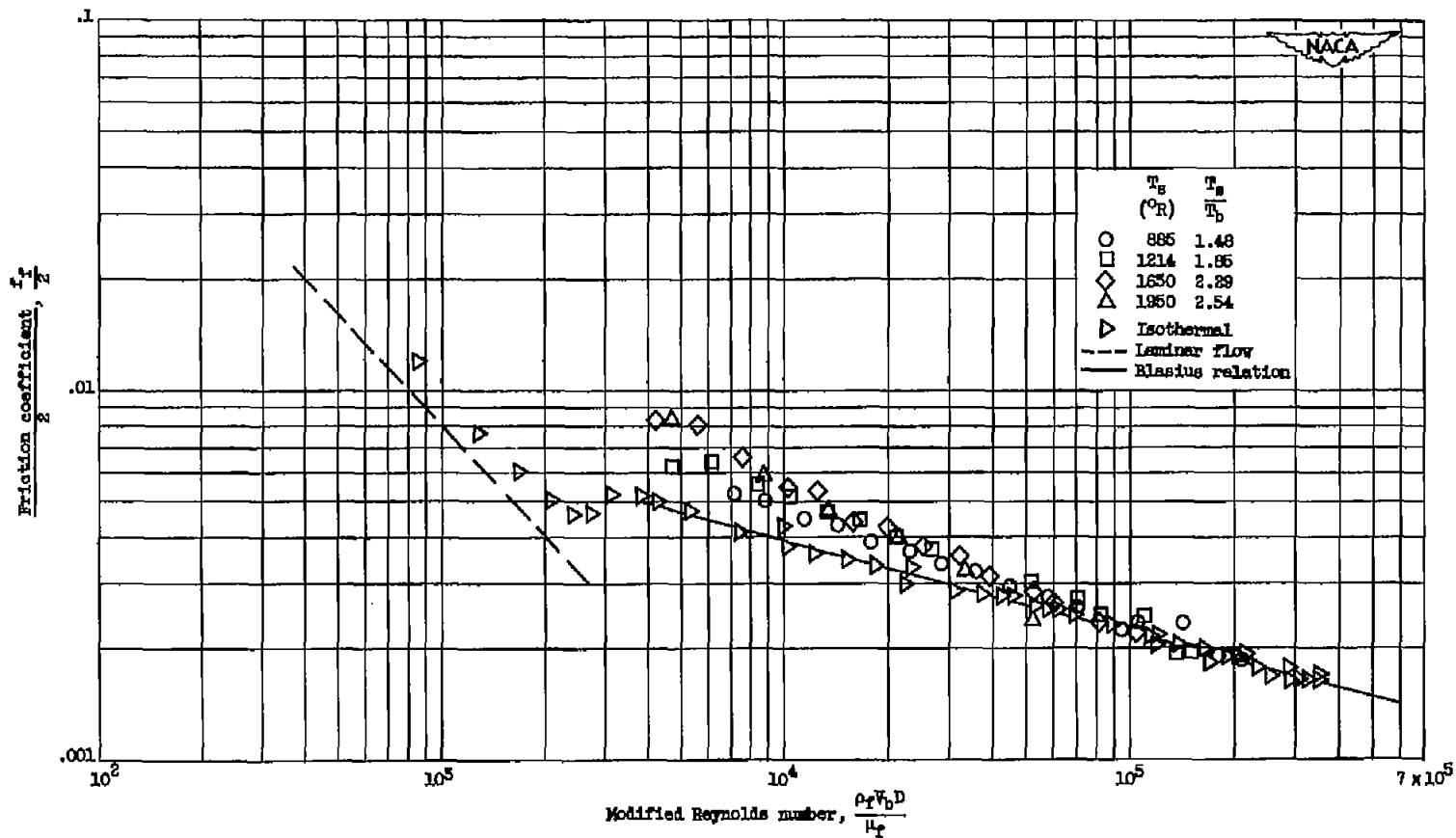
(a) Data for smooth tube. Conventional roughness ratio,  $e/r$ , 0.

Figure 13. - Correlation of bulk friction coefficients with bulk Reynolds number for tube with heat addition.



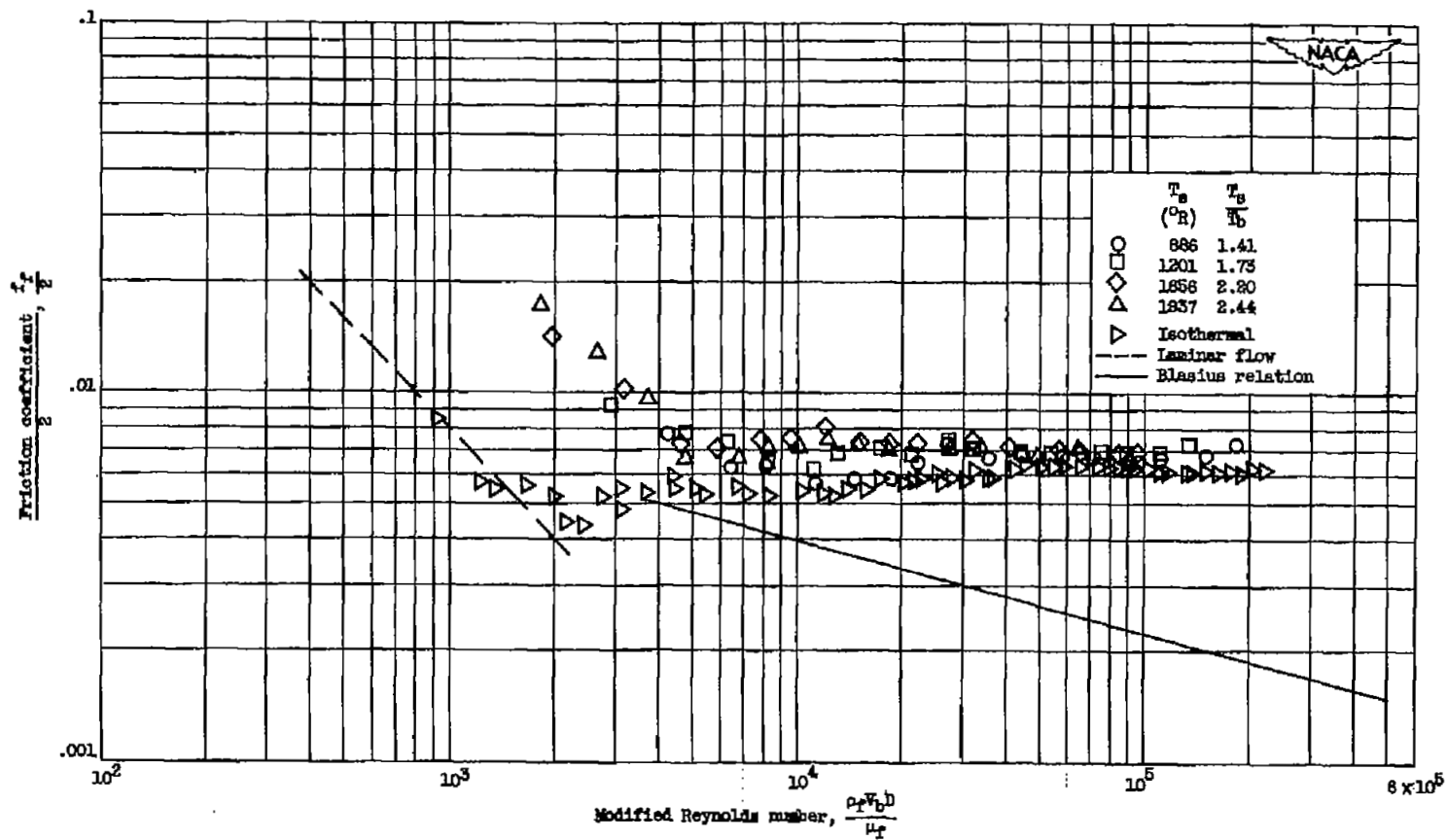
(b) Data for rough tube A. Conventional roughness ratio,  $e/x$ , 0.025.

Figure 13. - Concluded. Correlation of bulk friction coefficients with bulk Reynolds number for tube with heat addition.



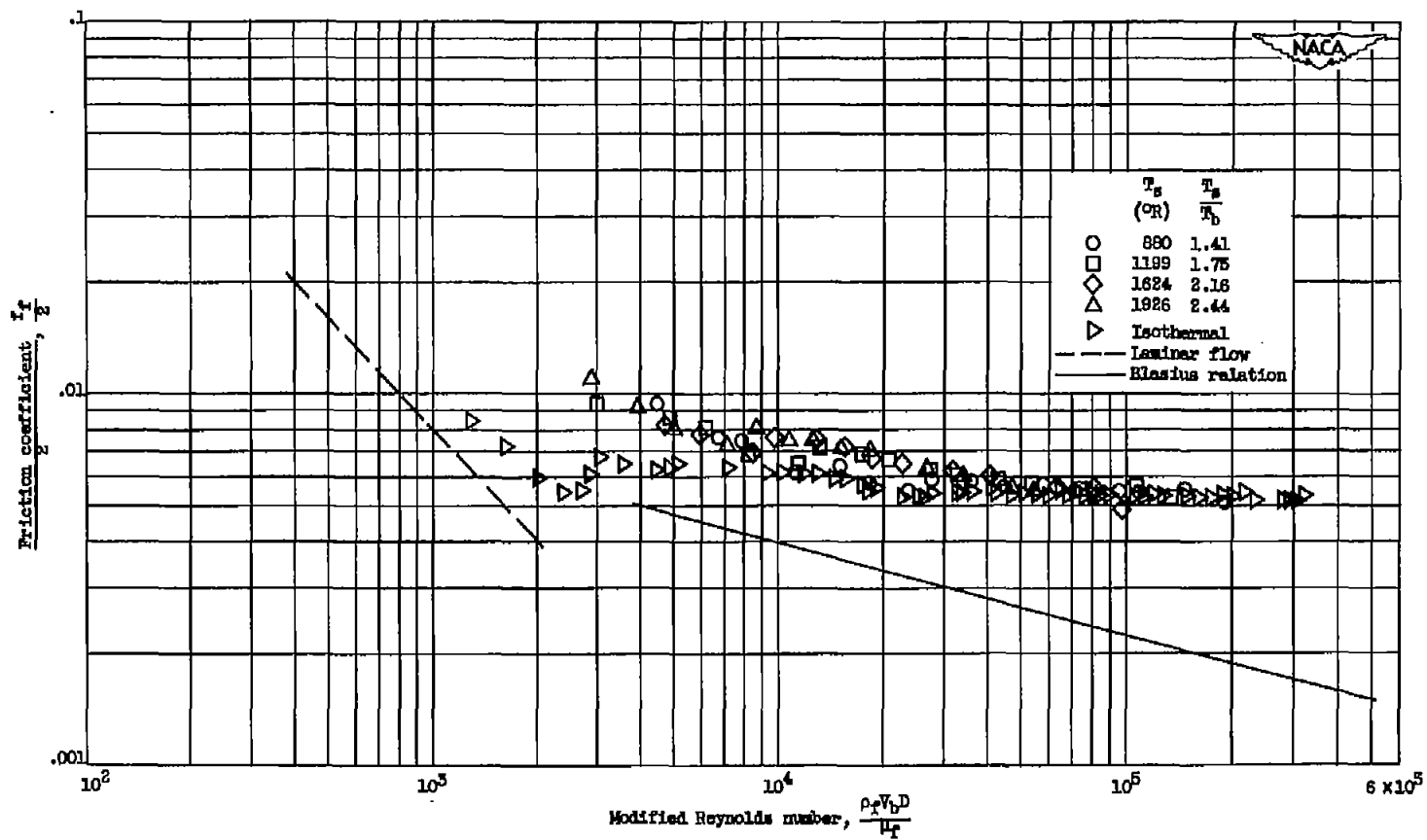
(a) Data for smooth tube. Conventional roughness ratio,  $e/x$ , 0.

Figure 14. - Correlation of film friction coefficients with modified film Reynolds number for tube with heat addition.



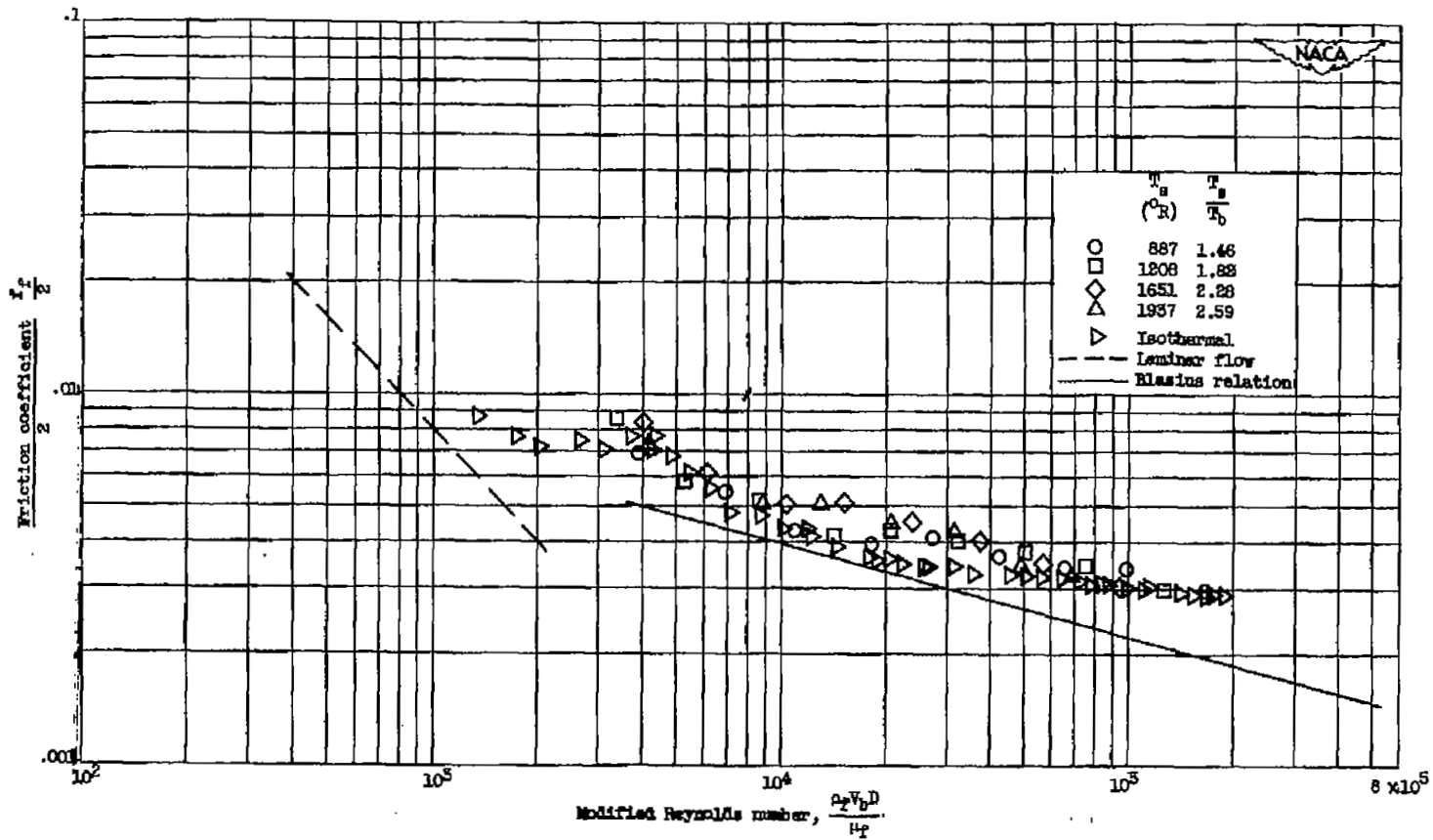
(b) Data for rough tube A. Conventional roughness ratio,  $e/r$ , 0.025.

Figure 14. - Continued. Correlation of film friction coefficients with modified film Reynolds number for tube with heat addition.



(a) Data for rough tube B. Conventional roughness ratio,  $e/r$ , 0.037.

Figure 14. - Continued. Correlation of film friction coefficients with modified film Reynolds number for tube with heat addition.



(d) Data for rough tube C. Conventional roughness ratio,  $e/r$ , 0.016.

Figure 14. - Concluded. Correlation of film friction coefficients with modified film Reynolds number for tube with heat addition.

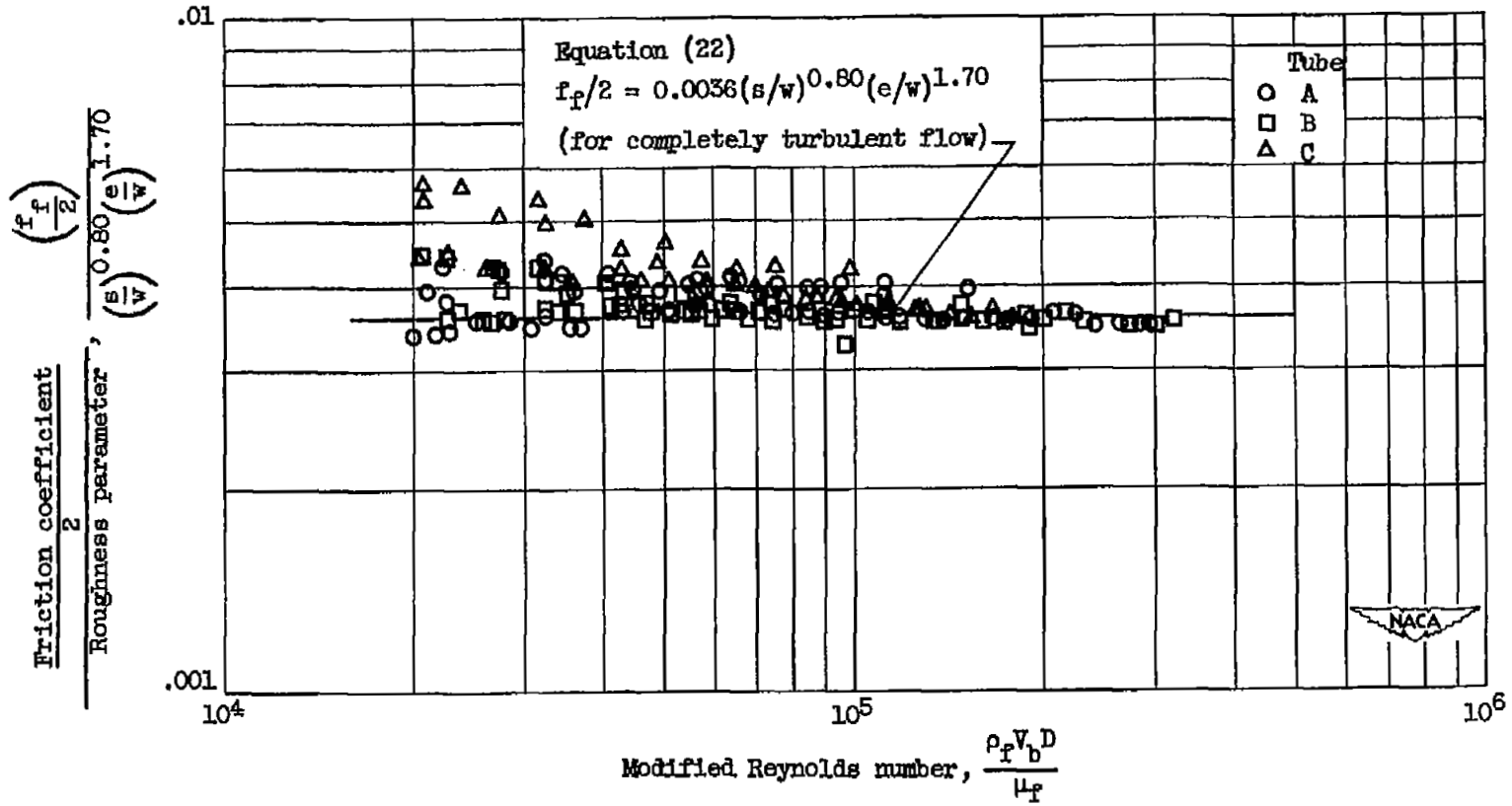


Figure 15. - Correlation of friction data for rough tubes A, B, and C with and without heat addition. Correlation strictly applicable only in complete turbulence region; hence, data restricted to values of  $\rho_f V_b D / \mu_f$  greater than 20,000 for tubes investigated herein.